On the polarization puzzles in the D^0 decays into vector meson pairs

Qiang Zhao

Division of Theoretical Physics

Institute of High Energy Physics, CAS

zhaoq@ihep.ac.cn

Work in collaboration with Ye CAO (曹叶) and Yin CHENG (程茵)

中国科学技术大学彭桓武高能基础理论研究中心，中国科学技术大学交叉学科理论研究中心
2024.03.21.

Outline

1. Background
2. Puzzling issues with the present experimental measurements of $D^0 \to VV$
3. Tree-level short-distance transitions vs. long-distance final state interactions
4. Some insights into D meson decays

Y. Cao, Y. Cheng and Q. Zhao, *Resolving the polarization puzzles in $D^0\to VV$*, [arXiv:2303.00535 [hep-ph]]

Y. Cao and Q. Zhao, *Study of weak radiative decays of $D^0\to V \gamma$*, [arXiv:2311.05249 [hep-ph]]

1. Background

Flavor physics provides a special testing ground for the SM and an important probe for new physics BSM.

In principle, for the non-leptonic hadronic two-body decays of $B \to MM$, systematic expansions in terms of Λ_{QCD}/m_b can be achieved.

- **QCD factorization (QCDF)**

[M. Beneke et al., PRL83, 1914 (1999); NPB591, 313 (2000)…]

- **Soft-collinear effective theory (SCET)**

[J. Chay et al., NPB680, 302 (2004); C. W. Bauer et al., PRD70, 054015 (2004); A. Williamson and J. Zupan, PRD74, 014003 (2006)…]

- **pQCD**

[Y.-Y. Keum, H.-n. Li, and A. Sanda, PLB504, 6 (2001); , PRD63, 054008 (2001); C.-D. Lu, K. Ukai, and M.-Z. Yang, PRD63, 074009 (2001), …]

Recognition of the helicity suppression on the short-distance weak annihilation amplitudes (couplings)

√: heli. favored

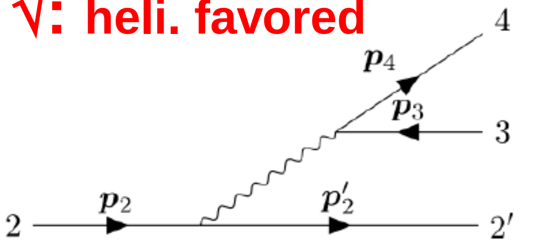

×: heli. suppressed

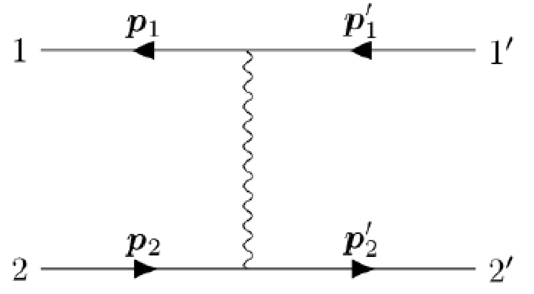

For the exclusive decay of heavy-flavor hadron, the longitudinal polarization fraction is defined as

$$f_L \equiv \frac{BR^{longi}}{BR^{longi} + BR^{trans}}$$

The longitudinal polarization dominance (LPD) means $f_L \simeq 1$.

- $B \to VV$:

In most cases, the exp. measurements support the **LPD** phenomenon, e.g. $B^0 \to \rho^+\rho^-, B^+ \to \rho^0\rho^+, \rho^0 K^{*+}$. But tensions exit in $B \to \phi K^*$.

Bernard Aubert et al., PRL91,171802 (2003)

K. F. Chen et al., PRL91, 201801 (2003).

- $D \to VV$:

Most literatures focus on the search for NP in $D^0 - \bar{D}^0$ mixing.

Apparent deviations of the **LPD** are observed in experiment.

A. N. Kamal et al., PRD43, 843 (1991)
Ian Hinchlie and Thomas A. Kaeding, PRD54, 914 (1996)
Paulo F. Bedaque et al., PRD49, 269 (1994)
Manfred Bauer, B. Stech, and M. Wirbel, Z. Phys. C34, 103 (1987)
Hai-Yang Cheng and Cheng-Wei Chiang, PRD81, 114020 (2010)
Hua-Yu Jiang, Fu-Sheng Yu, Qin Qin, Hsiang-nan Li, and Cai-Dian Lyu, Chin. Phys. C42, 063101 (2018)
Hai-Yang Cheng and Cheng-Wei Chiang, arXiv:2401.06316 [hep-ph]

Any tension with the SM needs a better understanding of the underlying non-perturbative dynamics.

But how to quantify it?

2. Puzzling issues with the present experimental measurements of $D^0 \to VV$

Polarization puzzles with $D^0 \to \phi\rho^0$ and $\phi\omega$

At the leading order, one would expect $Br(D^0 \to \phi\rho^0) \simeq Br(D^0 \to \phi\omega)$

$$u\bar{u} = \frac{1}{2}(u\bar{u} + d\bar{d}) + \frac{1}{2}(u\bar{u} - d\bar{d}) = \frac{1}{\sqrt{2}}(\omega + \rho^0)$$

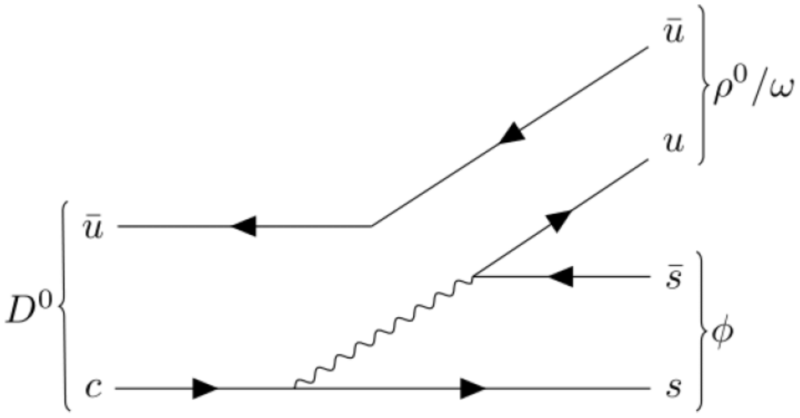

However, significant differences arise from the experimental measurements:

(I) Negligibly small longitudinal polarization with the $\phi\omega$ channel:

$$f_L = 0.00 \pm 0.10 \pm 0.08$$

which corresponds to $f_L < 0.24$ at 95% C.L.

(II) Dominance of the S-wave in $D^0 \to \phi\rho^0$ suggests relatively large longitudinal pola. fraction f_L.

(III) Difference in b.r.s:

$$Br^{exp}(D^0 \to \phi\rho^0) = (1.56 \pm 0.13) \times 10^{-3}$$

$$Br^{exp}(D^0 \to \phi\omega) \simeq (0.65 \pm 0.10) \times 10^{-3}$$

in unit of $(\times 10^{-3})$

$\phi\rho^0$	**S**	1.40 ± 0.12[21]
	P	0.08 ± 0.04[21]
	D	0.08 ± 0.03[21]
	T	-
	L	-
	Total	1.56 ± 0.13[21]
$\phi\omega$	T	0.65 ± 0.10[20]
	L	~ 0 [20]
	Total	0.65 ± 0.10[20]

There must be mechanisms beyond the leading tree-level transitions!

[20] M. Ablikim et al., BESIII Colla., Phys. Rev. Lett., 128, 011803 (2022)

[21] P. d'Argent et al., JHEP, 05:143 (2017)

Parametrizing the short-distance transition mechanisms

- **Cabibbo-favored (CF) decays $(\sim V_{cs}V_{ud})$ via color suppressed transitions:**

Γ_{75}	$\overline{K}^*(892)^0\rho^0$, $\overline{K}^{*0} \to K^-\pi^+$	(1.01 ± 0.05) %
Γ_{76}	$\overline{K}^*(892)^0\rho^0$ transverse, $\overline{K}^{*0} \to K^-\pi^+$	(1.2 ± 0.4) %
Γ_{90}	$\overline{K}^*(892)^0\omega$, $\overline{K}^{*0} \to K^-\pi^+$, $\omega \to \pi^+\pi^-\pi^0$	$(6.5 \pm 3.0) \times 10^{-3}$
Γ_{114}	$\overline{K}^*(892)^0\omega$	(1.1 ± 0.5) %

CS emission

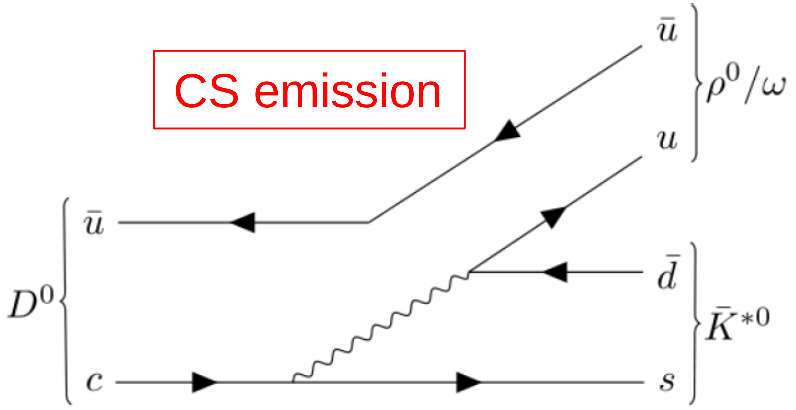

$$u\bar{u} = \frac{1}{2}(u\bar{u} + d\bar{d}) + \frac{1}{2}(u\bar{u} - d\bar{d}) = \frac{1}{\sqrt{2}}(\omega + \rho^0)$$

$$d\bar{d} = \frac{1}{2}(u\bar{u} + d\bar{d}) - \frac{1}{2}(u\bar{u} - d\bar{d}) = \frac{1}{\sqrt{2}}(\omega - \rho^0)$$

IC transition

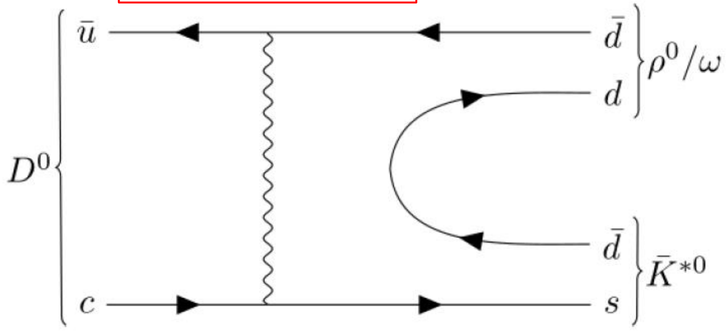

B.R. differences can be possibly accounted for by the interferences between the color suppressed emission (**CS**) and internal conversion (**IC**) transitions.

The CF decay of $D^0 \to K^{*-}\rho^+$ with the direct W emission (DE) has not been precisely measured in experiment!

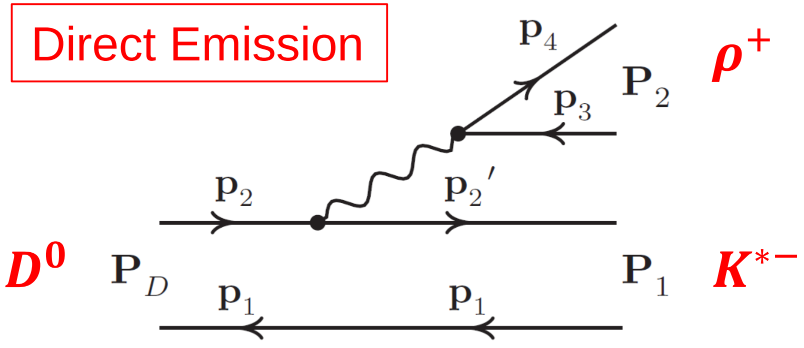

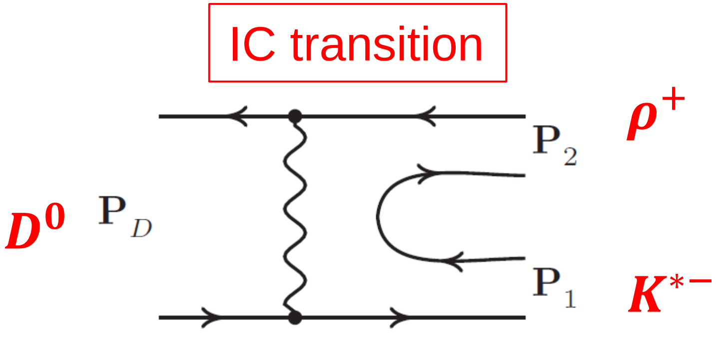

$$BR(D^0 \to K^{*-}\rho^+) = (6.5 \pm 2.5)\ \% \sim 5 \times BR(D^0 \to K^{*0}\rho^0)$$

H. Albrecht et al., New results on D0 decays, Z. Phys. C56, 7 (1992)

Decay channels	Amplitudes
$K^{*-}\rho^+$	$[g^{(P)}_{DE} + e^{i\theta} g^{(P)}_{IC(s\bar{d})}]V_{cs}V_{ud}$
$\bar{K}^{*0}\rho^0$	$\frac{1}{\sqrt{2}}[g^{(P)}_{CS} - e^{i\theta} g^{(P)}_{IC(s\bar{d})}]V_{cs}V_{ud}$
$\bar{K}^{*0}\omega$	$\frac{1}{\sqrt{2}}[g^{(P)}_{CS} + e^{i\theta} g^{(P)}_{IC(s\bar{d})}]V_{cs}V_{ud}$

- The CF decay amplitudes can be parametrized out by topological diagrams for the DE, CS, and IC transitions.
- θ is a trivial phase angle which prefers $\theta = 180°$.

Topological diagram approach (TDA):

Y. Kohara, PRD44, 2799 (1991); L.L. Chau, H.Y. Cheng and B. Tseng, PRD54, 2132 (1996); X.G. He and W. Wang, CPC42, 103108 (2018)

- **Singly Cabibbo suppressed (SCS) decays $(\sim V_{cs}V_{us}/\,V_{cd}V_{ud})$:**

Transition amplitude:

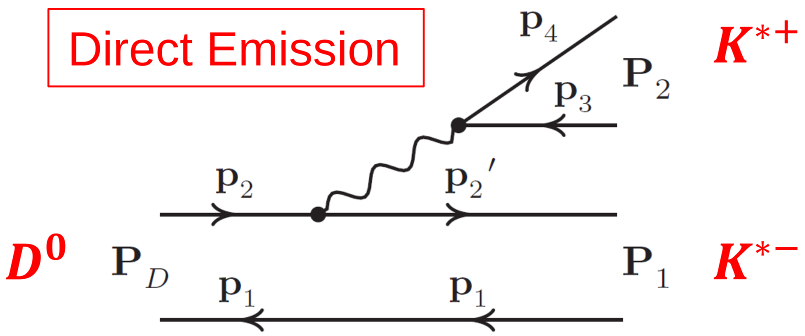

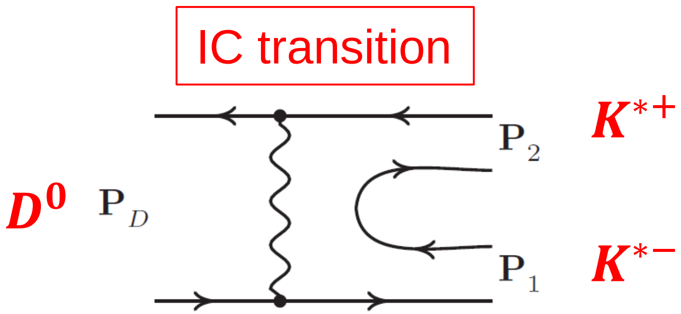

$$[g_{\rm DE}^{(\rm P)} + e^{i\theta} g_{{\rm IC}(s\bar{s})}^{(\rm P)}]V_{cs}V_{us}$$

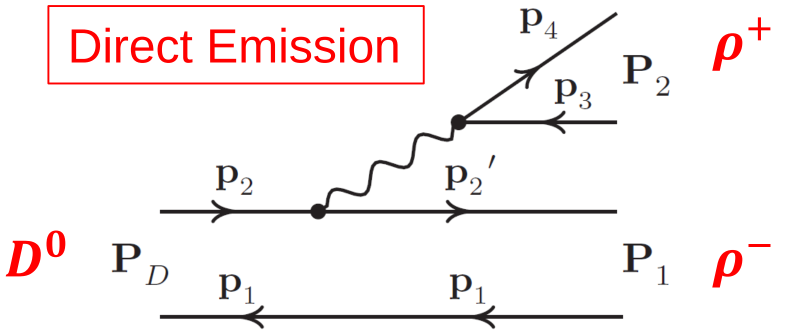

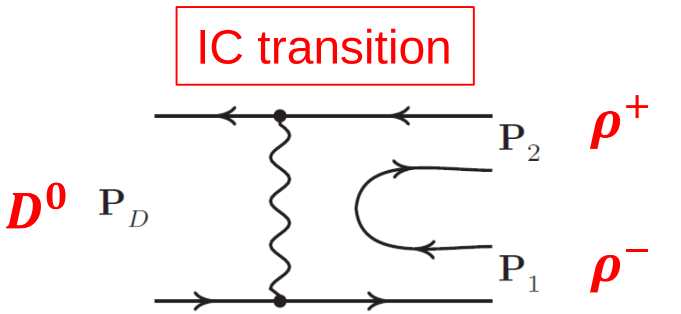

$$[g_{\rm DE}^{(\rm P)} + e^{i\theta} g_{{\rm IC}(d\bar{d})}^{(\rm P)}]V_{cd}V_{ud}$$

The SCS decays of $D^0 \to K^{*+}K^{*-}$ and $\rho^+\rho^-$, which is the only one involving the dominant DE transitions among the SCS decays, have NOT been measured in experiment!

The neutral decay channels involves the CS emissions and IC transitions:

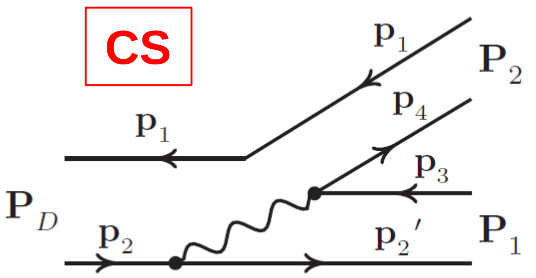

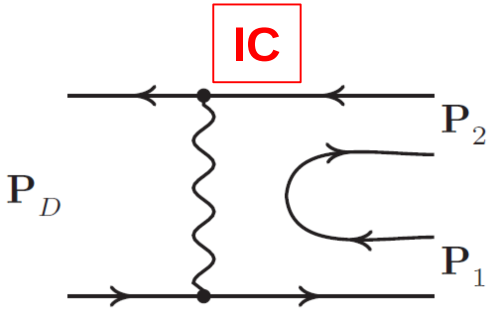

Decay channels	Amplitudes	
$K^{*+}K^{*-}$	$[g_{\rm DE}^{(\rm P)}+e^{i\theta}g_{{\rm IC}(s\bar{s})}^{(\rm P)}]V_{cs}V_{us}$	DE+IC
$K^{*0}\bar{K}^{*0}$	$e^{i\theta}[g_{{\rm IC}(s\bar{s})}^{(\rm P)}V_{cs}V_{us}+g_{{\rm IC}(d\bar{d})}^{(\rm P)}V_{cd}V_{ud}]$	
$\rho^+\rho^-$	$[g_{\rm DE}^{(\rm P)}+e^{i\theta}g_{{\rm IC}(d\bar{d})}^{(\rm P)}]V_{cd}V_{ud}$	
$\rho^0\rho^0$	$\frac{1}{2}[-g_{\rm CS}^{(\rm P)}+e^{i\theta}g_{{\rm IC}(d\bar{d})}^{(\rm P)}]V_{cd}V_{ud}$	CS+IC
$\omega\omega$	$\frac{1}{2}[g_{\rm CS}^{(\rm P)}+e^{i\theta}g_{{\rm IC}(d\bar{d})}^{(\rm P)}]V_{cd}V_{ud}$	
$\rho^0\omega$	$-\frac{1}{2}e^{i\theta}g_{{\rm IC}(d\bar{d})}^{(\rm P)}V_{cd}V_{ud}$	IC
$\phi\rho^0$	$\frac{1}{\sqrt{2}}g_{\rm CS}^{(\rm P)}V_{cs}V_{us}$	CS
$\phi\omega$	$\frac{1}{\sqrt{2}}g_{\rm CS}^{(\rm P)}V_{cs}V_{us}$	

in unit of $(\times 10^{-3})$

$K^{*0}\bar{K}^{*0}$	**S**	0.50 ± 0.03[21]
	P	0.27 ± 0.02[21]
	D	0.11 ± 0.01[21]
	T	-
	L	-
	Total	0.88 ± 0.04[21]
$\rho^+\rho^-$	T	-
	L	-
	Total	-
$\rho^0\rho^0$	**S**	0.18 ± 0.13[21]
	P	0.53 ± 0.13[21]
	D	0.62 ± 0.30[21]
	T	0.56 ± 0.07[19]
	L	1.27 ± 0.10[19]
	Total	1.85 ± 0.13[19]
		1.33 ± 0.35[21]
$\omega\omega$	T	-
	L	-
	Total	-
$\rho^0\omega$	T	-
	L	-
	Total	-
$\phi\rho^0$	**S**	1.40 ± 0.12[21]
	P	0.08 ± 0.04[21]
	D	0.08 ± 0.03[21]
	T	-
	L	-
	Total	1.56 ± 0.13[21]
$\phi\omega$	T	0.65 ± 0.10[20]
	L	~ 0 [20]
	Total	0.65 ± 0.10[20]

[19] J. M. Link et al., FOCUS Colla., Phys. Rev. D, 75:052003, 2007

[20] M. Ablikim et al., BESIII Colla., Phys. Rev. Lett., 128(1):011803, 2022

[21] P. d'Argent et al., JHEP, 05:143, 2017

- Notice that there exist significant differences between the $K^{*+}K^{*-}$ and $K^{*0}\overline{K}^{*0}$ channels.

$K^{*+}K^{*-}$	$[g^{(P)}_{DE} + e^{i\theta} g^{(P)}_{IC(s\bar{s})}]V_{cs}V_{us}$
$K^{*0}\bar{K}^{*0}$	$e^{i\theta}[g^{(P)}_{IC(s\bar{s})}V_{cs}V_{us} + g^{(P)}_{IC(d\bar{d})}V_{cd}V_{ud}]$

$$BR(D^0 \to K^{*+}K^{*-}) \gg BR(D^0 \to K^{*0}\overline{K}^{*0})$$

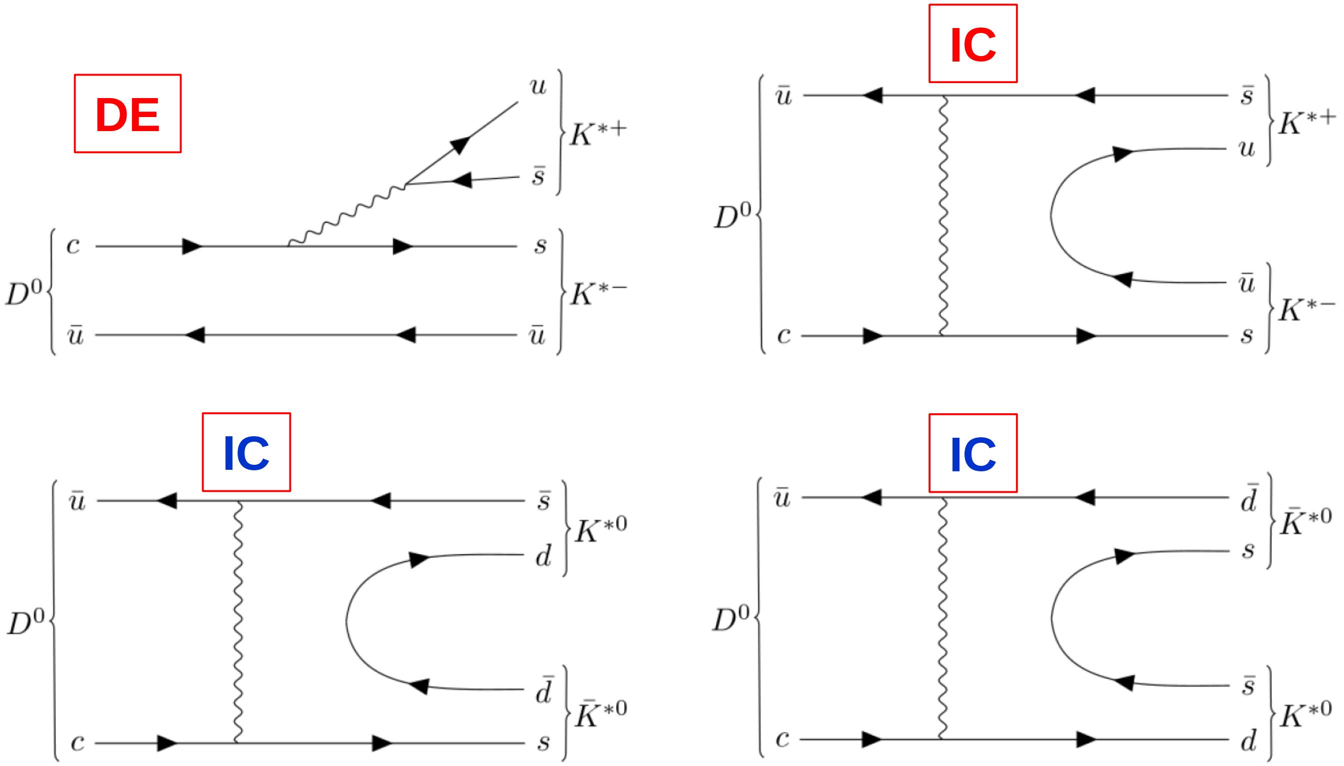

- Long distance transition mechanism due to the $K^*\overline{K}^*$ final-state interactions (FSIs) should be considered:

$$2m_{K^*} \sim m_\phi + m_\rho \sim m_\phi + m_\omega$$

- Moreover, FSIs involving other intermediate meson rescatterings can also contribute. A systematic treatment is required.

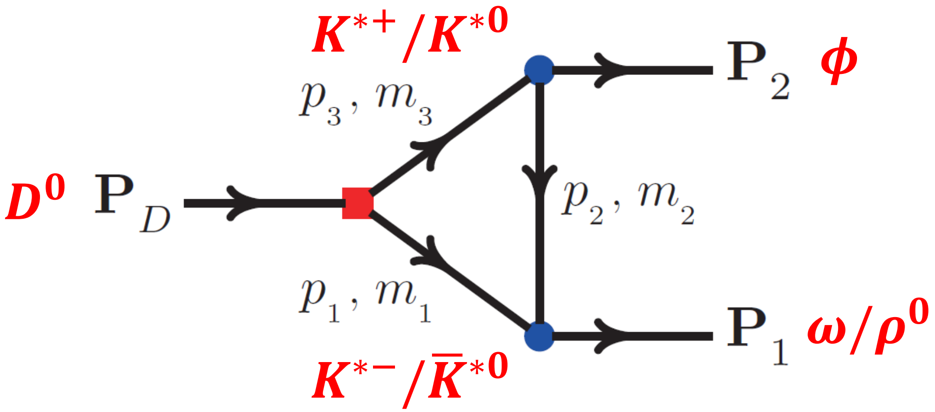

Why final state interactions (FSIs)?

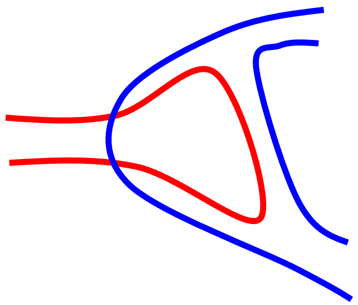

$\psi(3770) \to non D\bar{D}$

"ρπ puzzle"

Y.J. Zhang, G. Li, Q. Zhao, PRL(2009);
X. Liu, B. Zhang, X.Q. Li, PLB(2009)
Q. Wang et al. PRD(2012), PLB(2012)

$\chi_{c1} \to VV, \ \chi_{c2} \to VP$

X.-H. Liu et al, PRD81, 014017(2010);
X. Liu et al, PRD81, 074006(2010)

$\eta_c(\eta_c') \to VV$

Q. Wang et al, PRD2012

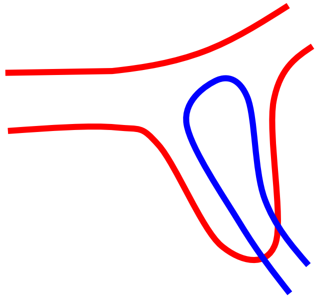

$\psi' \to J/\psi\pi^0, \psi' \to J/\psi\eta$

$\psi' \to \gamma\eta_c, J/\psi \to \gamma\eta_c$

G. Li and Q. Zhao, PRD(2011)074005

F.K. Guo, C. Hanhart, G. Li, U.-G. Meiβner and Q. Zhao, PRD82, 034025 (2010); PRD83, 034013 (2011)

F.K. Guo and Ulf-G Meiβner, PRL108(2012)112002

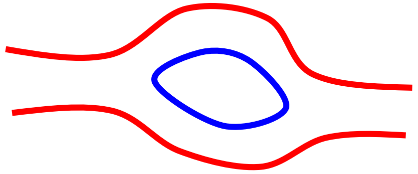

$D_{s1}(2460) - D_{s1}(2536)$

The mass shift in charmonia and charmed mesons, E.Eichten et al., PRD17(1987)3090

X.-G. Wu and Q. Zhao, PRD85, 034040 (2012)

1. New effective D.o.F. can be introduced near threshold via FSIs

2. Triangle singularity brings novel structures

Exotics of Type-III:
Peak structures caused by kinematic effects, in particular, by triangle singularity.

$$\Gamma_3(s_1,s_2,s_3) = \frac{1}{i(2\pi)^4}\int \frac{d^4q_1}{(q_1^2-m_1^2+i\epsilon)(q_2^2-m_2^2+i\epsilon)(q_3^2-m_3^2+i\epsilon)}$$
$$= \frac{-1}{16\pi^2}\int_0^1\int_0^1\int_0^1 da_1\, da_2\, da_3\, \frac{\delta(1-a_1-a_2-a_3)}{D-i\epsilon},$$

$$D \equiv \sum_{i,j=1}^{3} a_i a_j Y_{ij},\quad Y_{ij} = \frac{1}{2}\left[m_i^2+m_j^2-(q_i-q_j)^2\right]$$

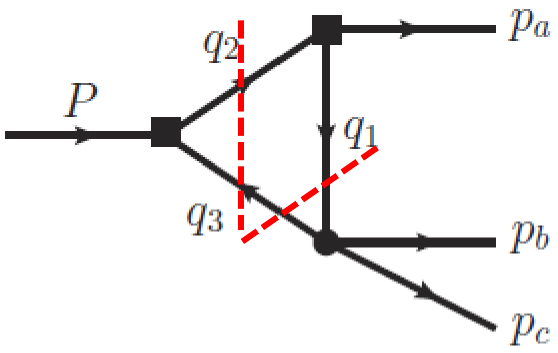

The TS occurs when all the three internal particles can approach their on-shell condition simultaneously:

$\partial D/\partial a_j = 0$ for all j=1,2,3. ⇨ $\det[Y_{ij}] = 0$

L. D. Landau, Nucl. Phys. 13, 181 (1959);
J.J. Wu, X.-H. Liu, Q. Zhao, B.-S. Zou, Phys. Rev. Lett. 108, 081003 (2012);
Q. Wang, C. Hanhart, Q. Zhao, Phys. Rev. Lett. 111, 132003 (2013); Phys. Lett. B 725, 106 (2013)
X.-H. Liu, M. Oka and Q. Zhao, PLB753, 297(2016);
F.-K. Guo, C. Hanhart, U.-G. Meissner, Q. Wang, Q. Zhao, B.-S. Zou, arXiv:1705.00141[hep-ph], Rev. Mod. Phys. 90, 015004 (2018)

3. Tree-level short-distance transitions vs. long-distance final state interactions

- Taking $D^0 \to \phi\rho^0/\phi\omega$ as an example, the tree-level amplitude reads:

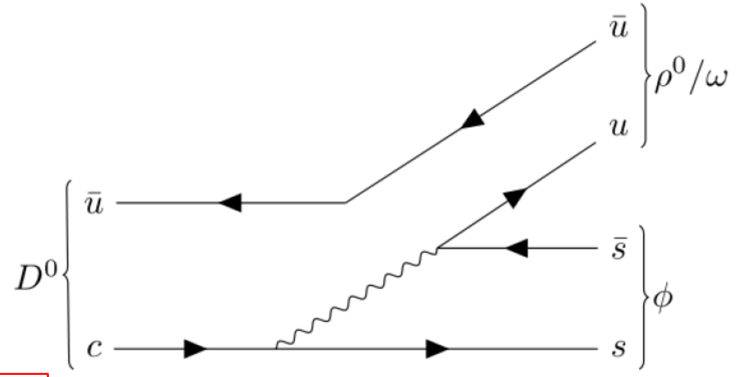

$$i\mathcal{M}_{(\mathrm{P})}(D^0 \to \phi\rho^0/\phi\omega)$$
$$= \langle \phi\rho^0/\phi\omega|\phi(u\bar{u})\rangle\langle\phi(u\bar{u})|H_{W(\mathrm{P})}^{(\mathrm{CS})}|D_0\rangle = \frac{1}{\sqrt{2}} g_{\mathrm{CS}}^{(\mathrm{P})} V_{cs} V_{us}$$

To be calculated explicitly in the NRCQM

- The amplitude due to the intermediate $K^{*+}K^{*-}$ rescatterings can be written as:

$$i\mathcal{M}_{(\mathrm{P})\phi\rho^0}^{loop} = \frac{1}{\sqrt{2}} g_{\mathrm{DE}}^{(\mathrm{P})} V_{cs} V_{us} \sum_{(\mathbb{K})} \tilde{\mathcal{I}}[(\mathrm{P}); K^{*+}, K^{*-}, (\mathbb{K})]$$

$$i\mathcal{M}_{(\mathrm{P})\phi\omega}^{loop} = \left(\frac{1}{\sqrt{2}} g_{\mathrm{DE}}^{(\mathrm{P})} + e^{i\delta} g_{\mathrm{IC}(s\bar{s})}^{(\mathrm{P})}\right) V_{cs} V_{us} \times \sum_{(\mathbb{K})} \tilde{\mathcal{I}}[(\mathrm{P}); K^{*+}, K^{*-}, (\mathbb{K})] \,,$$

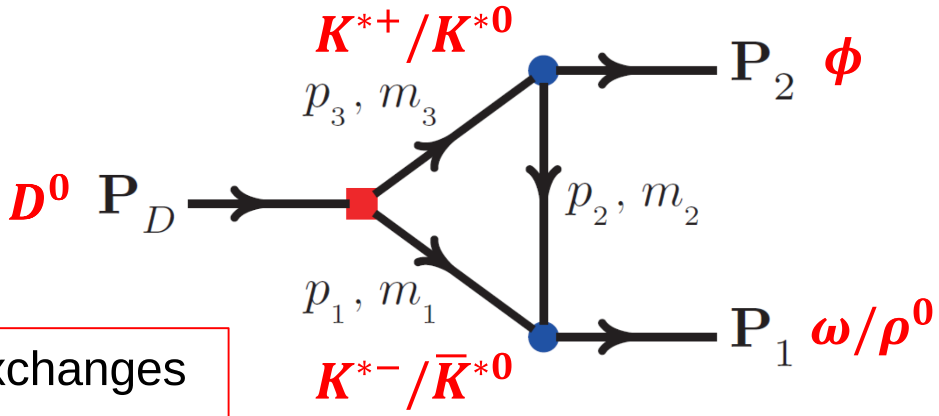

"P" can be either "PC" or "PV" for parity-conserving or parity-violating amplitudes.

Different strange particle exchanges in $K^{*+}K^{*-} \to \phi\rho^0/\phi\omega$.

Tree-level amplitudes in the NRCQM

The non-relativistic constituent quark model (NRCQM) for the tree-level amplitudes:

The effective weak Hamiltonian: $$H_W = \frac{G_F}{\sqrt{2}} \int \mathrm{d}\boldsymbol{x} \, \frac{1}{2}\{J^{-,\mu}(\boldsymbol{x}), J^{+}_{\mu}(\boldsymbol{x})\},$$

where

$$J^{+,\mu}(\boldsymbol{x}) = (\bar{u} \;\; \bar{c}) \cdot \gamma^{\mu}(1-\gamma_5) \cdot \begin{pmatrix} \cos\theta_C & -\sin\theta_C \\ \sin\theta_C & \cos\theta_C \end{pmatrix} \cdot \begin{pmatrix} d \\ s \end{pmatrix},$$

$$J^{-,\mu}(\boldsymbol{x}) = (\bar{d} \;\; \bar{s}) \cdot \begin{pmatrix} \cos\theta_C & -\sin\theta_C \\ \sin\theta_C & \cos\theta_C \end{pmatrix} \cdot \gamma^{\mu}(1-\gamma_5) \cdot \begin{pmatrix} u \\ c \end{pmatrix}.$$

(1 → 3)

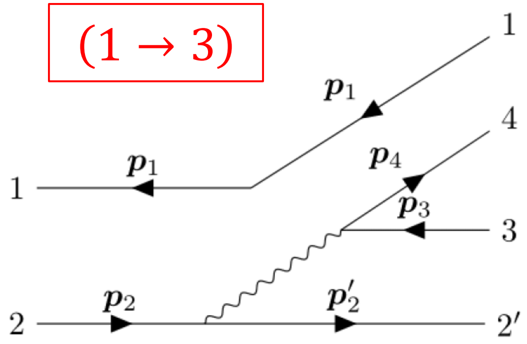

The operators for the W emission and internal W exchange are:

$$H_{W,1\to 3} = \frac{G_F}{\sqrt{2}} V_{q_2 q_2'} V_{q_3 q_4} \frac{1}{(2\pi)^3} \delta^3(\boldsymbol{p}_2 - \boldsymbol{p}_2' - \boldsymbol{p}_3 - \boldsymbol{p}_4)$$
$$\times \bar{u}(\boldsymbol{p}_2', m_2')\gamma_{\mu}(1-\gamma_5)u(\boldsymbol{p}_2, m_2)\bar{u}(\boldsymbol{p}_4, m_4)\gamma^{\mu}(1-\gamma_5)v(\boldsymbol{p}_3, m_3),$$
$$H_{W,2\to 2} = \frac{G_F}{\sqrt{2}} V_{q_2 q_2'} V_{q_1 q_1'} \frac{1}{(2\pi)^3} \delta^3(\boldsymbol{p}_1 + \boldsymbol{p}_2 - \boldsymbol{p}_1' - \boldsymbol{p}_2')$$
$$\times \bar{u}(\boldsymbol{p}_2', m_2')\gamma_{\mu}(1-\gamma_5)u(\boldsymbol{p}_2, m_2)\bar{v}(\boldsymbol{p}_1, m_1)\gamma^{\mu}(1-\gamma_5)v(\boldsymbol{p}_1', m_1).$$

(2 → 2)

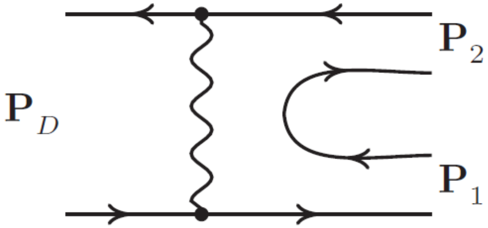

A. Le Yaouanc, L. Oliver, O. Pene, and J. C. Raynal. HADRON TRANSITIONS IN THE QUARK MODEL. 1988

The operator can be expressed as

$$H_I \equiv C \sum_n \hat{O}_n,$$

where $\hat{O}_n = \hat{O}^{flavor} \hat{O}^{color} \hat{O}_n^{spin} \hat{O}_n^{spatial}$

Advantages of the NRCQM approach:

The SU(3) flavor symmetry breaking is embedded in the NRCQM w.f. and operators. Namely, the weak couplings defined for each topological diagram may have different values in different processes.

The transition amplitude reads

$$\langle M'(J_f^{P_f}; \boldsymbol{P}_f; J_f, M_{J_f}) | \hat{O}_n | M(J_i^{P_i}; \boldsymbol{P}_i; J_i, M_{J_i}) \rangle$$

$$= \sum_{M_{L_i}, M_{S_i}, M_{L_f}, M_{S_f}} \left[\langle \phi_f | \hat{O}^{flavor} | \phi_i \rangle \langle \chi_f^{S_f, M_{S_f}} | \hat{O}_n^{spin} | \chi_i^{S_i, M_{S_i}} \rangle \langle \psi_f^{N_f, L_f, M_{L_f}} | \hat{O}_n^{spatial} | \psi_i^{N_i, L_i, M_{L_i}} \rangle \right]$$

The wavefunction can be expressed as a mock state:

$$|M(J^P; \boldsymbol{P}_c; J, M_J)\rangle = \sum_{M_L, M_S} \langle L M_L S M_S | J M_J \rangle \int \mathrm{d}\boldsymbol{p}_1 \mathrm{d}\boldsymbol{p}_2 \, \delta^3(\boldsymbol{p}_1 + \boldsymbol{p}_2 - P_c) \psi_{NLM_L}(\boldsymbol{p}_1, \boldsymbol{p}_2) \phi_{i_1, i_2}$$
$$\chi_{s_1, s_2}^{S, S_z} \frac{\delta_{c_1, c_2}}{\sqrt{3}} b_{i_1, s_1, c_1, \boldsymbol{p}_1}^{\dagger} d_{i_2, s_2, c_2, \boldsymbol{p}_2}^{\dagger} |0\rangle,$$

For instance, the operators for the W emission $(1 \to 3)$ in the PC and PV transitions:

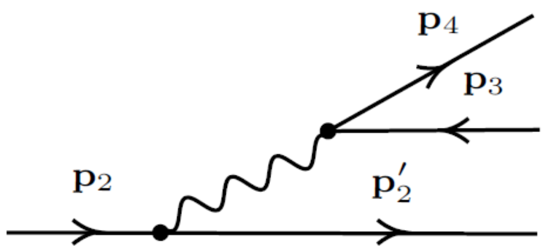

$$H^{PC}_{W,1\to 3} = \frac{G_F}{\sqrt{2}} V_{q_2 q_2'} V_{q_3 q_4} \frac{\beta}{(2\pi)^3} \delta^3(\boldsymbol{p}_2 - \boldsymbol{p}_2' - \boldsymbol{p}_3 - \boldsymbol{p}_4) \hat{O}_{color} \hat{O}_{flavor}$$
$$\times \{\langle s_2'|I|s_2\rangle\langle s_4\bar{s}_3|\boldsymbol{\sigma}|0\rangle \cdot (\frac{\boldsymbol{p}_3}{2m_3} + \frac{\boldsymbol{p}_4}{2m_4}) + \langle s_2'|\boldsymbol{\sigma}|s_2\rangle \cdot (\frac{\boldsymbol{p}_2}{2m_2} + \frac{\boldsymbol{p}_2'}{2m_2'})\langle s_4\bar{s}_3|I|0\rangle$$
$$- \langle s_4\bar{s}_3|\boldsymbol{\sigma}|0\rangle \cdot [\langle s_2'|I|s_2\rangle(\frac{\boldsymbol{p}_2}{2m_2} + \frac{\boldsymbol{p}_2\prime}{2m_2'}) - i\langle s_2'|\boldsymbol{\sigma}|s_2\rangle \times (\frac{\boldsymbol{p}_2}{2m_2} - \frac{\boldsymbol{p}_2'}{2m_2'})]$$
$$- \langle s_2'|\boldsymbol{\sigma}|s_2\rangle \cdot [(\frac{\boldsymbol{p}_3}{2m_3} + \frac{\boldsymbol{p}_4}{2m_4})\langle s_4\bar{s}_3|I|0\rangle - i\langle s_4\bar{s}_3|\boldsymbol{\sigma}|0\rangle \times (\frac{\boldsymbol{p}_3}{2m_3} - \frac{\boldsymbol{p}_4}{2m_4})]\},$$

$$H^{PV}_{W,1\to 3} = \frac{G_F}{\sqrt{2}} V_{q_2 q_2'} V_{q_3 q_4} \frac{\beta}{(2\pi)^3} \delta^3(\boldsymbol{p}_2 - \boldsymbol{p}_2' - \boldsymbol{p}_3 - \boldsymbol{p}_4) \hat{O}_{color} \hat{O}_{flavor}$$
$$\times \{-\langle s_2'|I|s_2\rangle\langle s_4\bar{s}_3|I|0\rangle + \langle s_2'|\boldsymbol{\sigma}|s_2\rangle \cdot \langle s_4\bar{s}_3|\boldsymbol{\sigma}|0\rangle\},$$

⇒

$$i\mathcal{M}_{(\mathrm{P})} \;=\; \langle V_1(\mathbf{P}_1; J_1, J_{1z}) V_2(\mathbf{P}_2; J_2, J_{2z})|\hat{H}^{(\mathrm{P})}_{W,1\to 3}|D^0(\mathbf{P}_D; J_i, J_{iz})\rangle \equiv g^{(\mathrm{P});J_{iz};J_{1z},J_{2z}}_{\mathrm{DE/CS}} V_{cq} V_{uq}$$

- A. Le Yaouanc, L. Oliver, O. Pene, and J. C. Raynal. HADRON TRANSITIONS IN THE QUARK MODEL. 1988
- J.-M. Richard, Q. Wang, and Q. Zhao, arXiv:1604.04208[nucl-th]
- P.-Y. Niu, J.-M. Richard, Q. Wang, and Q. Zhao, Phys. Rev. D102, 073005 (2020)
- P.-Y. Niu, Q. Wang, and Q. Zhao, Phys. Lett. B 826 (2022) 136916

The transition matrix element for the DE process can be written as

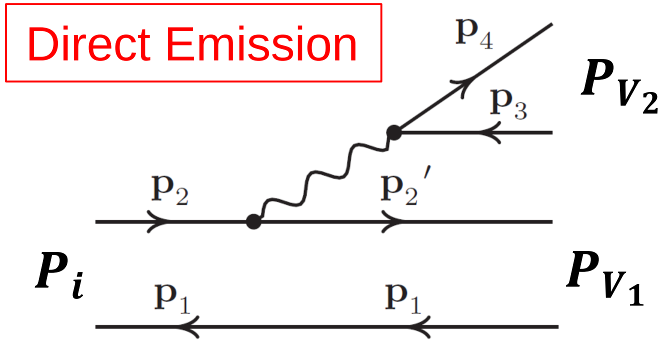

$$\mathcal{M}_{\mathrm{DE}}^{M_{J_{V_1}},M_{J_{V_2}}} = \langle M(1^-;\boldsymbol{P}_{V_1};1,M_{J_{V_1}})\, M(1^-;\boldsymbol{P}_{V_2};1,M_{J_{V_2}})|H_{W,1\to 3}|M(0^-;\boldsymbol{P}_i;0,0)\rangle$$

where the spatial integral is

$$\begin{aligned} I_{\mathrm{DE}} &= \langle \psi_{000}(\boldsymbol{P}_{V_1})\psi_{000}(\boldsymbol{P}_{V_2})|\hat{O}^{spatial}_{W,1\to 3}|\psi_{000}(\boldsymbol{P}_i)\rangle \\ &= \int \mathrm{d}\boldsymbol{p}_1\mathrm{d}\boldsymbol{p}_2\mathrm{d}\boldsymbol{p}_2'\mathrm{d}\boldsymbol{p}_3\mathrm{d}\boldsymbol{p}_4\psi^*_{000}(\boldsymbol{p}_1,\boldsymbol{p}_2')\delta^3(\boldsymbol{P}_{V_1}-\boldsymbol{p}_1-\boldsymbol{p}_2')\psi^*_{000}(\boldsymbol{p}_3,\boldsymbol{p}_4)\delta^3(\boldsymbol{P}_{V_2}-\boldsymbol{p}_3-\boldsymbol{p}_4) \\ &\times \hat{O}^{spatial}_{W,1\to 3}\psi_{000}(\boldsymbol{p}_1,\boldsymbol{p}_2)\delta^3(\boldsymbol{P}_i-\boldsymbol{p}_1-\boldsymbol{p}_2)\delta^3(\boldsymbol{p}_2-\boldsymbol{p}_3-\boldsymbol{p}_4-\boldsymbol{p}_2'). \end{aligned}$$

The transition matrix element for the CS process can be written as

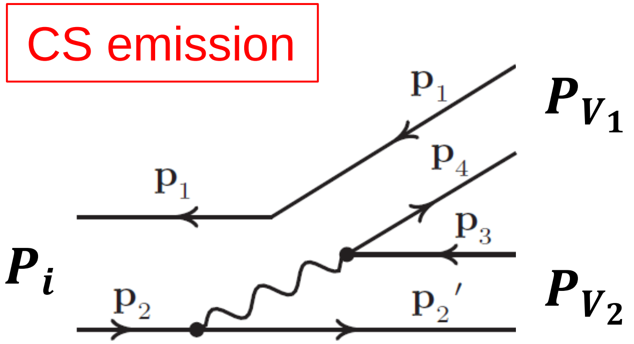

$$\mathcal{M}_{\mathrm{CS}}^{M_{J_{V_1}},M_{J_{V_2}}} = \langle M(1^-;\boldsymbol{P}_{V_1};1,M_{J_{V_1}})\, M(1^-;\boldsymbol{P}_{V_2};1,M_{J_{V_2}})|H_{W,1\to 3}|M(0^-;\boldsymbol{P}_i;0,0)\rangle.$$

where the spatial integral is

$$\begin{aligned} I_{\mathrm{CS}} &= \langle \psi_{000}(\boldsymbol{P}_{V_1})\psi_{000}(\boldsymbol{P}_{V_2})|\hat{O}^{spatial}_{W,1\to 3}|\psi_{000}(\boldsymbol{P}_i)\rangle \\ &= \int \mathrm{d}\boldsymbol{p}_1\mathrm{d}\boldsymbol{p}_2\mathrm{d}\boldsymbol{p}_2'\mathrm{d}\boldsymbol{p}_3\mathrm{d}\boldsymbol{p}_4\psi^*_{000}(\boldsymbol{p}_1,\boldsymbol{p}_4)\delta^3(\boldsymbol{P}_{V_1}-\boldsymbol{p}_1-\boldsymbol{p}_4)\psi^*_{000}(\boldsymbol{p}_3,\boldsymbol{p}_2')\delta^3(\boldsymbol{P}_{V_2}-\boldsymbol{p}_3-\boldsymbol{p}_2') \\ &\times \hat{O}^{spatial}_{W,1\to 3}\psi_{000}(\boldsymbol{p}_1,\boldsymbol{p}_2)\delta^3(\boldsymbol{P}_i-\boldsymbol{p}_1-\boldsymbol{p}_2)\delta^3(\boldsymbol{p}_2-\boldsymbol{p}_3-\boldsymbol{p}_4-\boldsymbol{p}_2'), \end{aligned}$$

Long-distance amplitudes via the FSIs

For instance, the loop amplitude for the kaon exchange can be expressed as

$$\tilde{\mathcal{I}}[(\mathrm{PC}); K^{*+}, K^{*-}, (K)]$$
$$= \int \frac{d^4 p_1}{(2\pi)^4} V_{1\mu\nu} D^{\mu\mu'}(K^*) V_{2\mu'} D(K) V_{3\nu'} D^{\nu\nu'}(\bar{K}^*) \mathcal{F}(p_i^2)$$

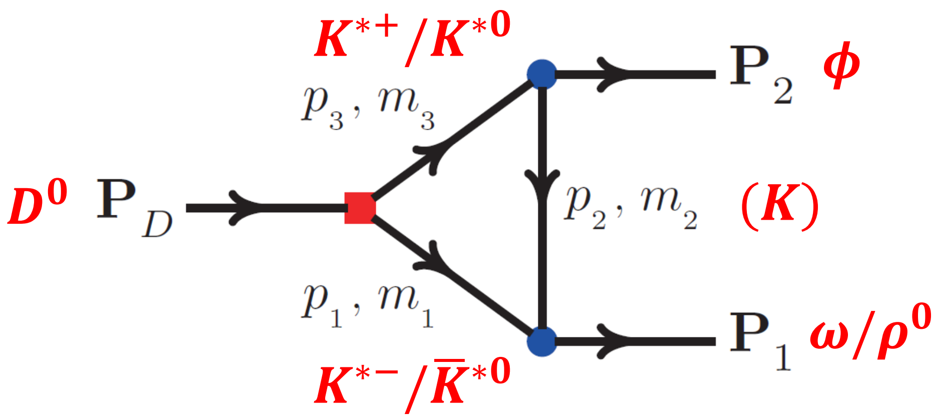

with the vertex couplings:

$$\begin{cases} V_{1\mu\nu} = -i g_{DK^*\bar{K}^*} \epsilon_{\alpha\beta\mu\nu} p_1^\alpha p_3^\beta, \\ V_{2\mu'} = i g_{V_1 K^* \bar{K}} \epsilon_{\alpha_1\beta_1\mu'\delta} p_1^{\alpha_1} p_{V_1}^{\beta_1} \varepsilon_{V_1}^{\delta *}, \\ V_{3\nu'} = i g_{V_2 \bar{K}^* K} \epsilon_{\alpha_2\beta_2\nu'\lambda} p_3^{\alpha_2} p_{V_2}^{\beta_2} \varepsilon_{V_2}^{\lambda *}, \end{cases}$$

and the propagators for the vector and pseudoscalar mesons:

$$\begin{cases} D^{\mu\mu'}(K^*) = -i(g^{\mu\mu'} - p^\mu p^{\mu'}/p^2)/(p^2 - m_{K^*}^2 + i\epsilon) \\ D(K) = i/(p^2 - m_K^2 + i\epsilon) \end{cases}$$

A form factor is introduced to cut off the UV divergence:

$$\mathcal{F}(p_i^2) = \prod_i \left(\frac{\Lambda_i^2 - m_i^2}{\Lambda_i^2 - p_i^2}\right),$$

with $\Lambda_i \equiv m_i + \alpha\Lambda_{QCD}$, and $\Lambda_{QCD} =$ 220 MeV, and $\alpha \simeq 1 \sim 2$.

P wave loop amplitudes:

- $[P,\ K^*,\ \bar{K}^*,\ (K^*)]$

  The amplitude for the $[P,\ K^*,\ \bar{K}^*,\ (K^*)]$ loop is:

$$i\mathcal{M}=\int\frac{d^4p_1}{(2\pi)^4}V_{1\mu\nu}D^{\mu\mu'}(K^*)V_{2\mu'\rho}D^{\rho\sigma}(K^*)V_{3\nu'\sigma}D^{\nu\nu'}(\bar{K}^*)\mathcal{F}(p_i^2),$$

$$V_{2\mu'\rho}=ig_{V_1K^*\bar{K}^*}[(p_1+p_{V_1})_\rho\varepsilon^{\delta*}_{V_1}g_{\mu'\delta}+(p_2-p_{V_1})_{\mu'}\varepsilon^{\delta*}_{V_1}g_{\delta\rho}-(p_1+p_2)_\delta\varepsilon^{\delta*}_{V_1}g_{\mu'\rho}],$$

$$V_{3\nu'\sigma}=-ig_{V_2K^*\bar{K}^*}[(p_3+p_{V_2})_\sigma\varepsilon^{\lambda*}_{V_2}g_{\nu'\lambda}-(p_2+p_{V_2})_{\nu'}\varepsilon^{\lambda*}_{V_2}g_{\lambda\sigma}+(p_2-p_3)_\lambda\varepsilon^{\lambda*}_{V_2}g_{\nu'\sigma}].$$

- $[P,\ K^*,\ \bar{K}^*,\ (\kappa)]$

  The amplitude for the $[P,\ K^*,\ \bar{K}^*,\ (\kappa)]$ loop is

$$i\mathcal{M}=\int\frac{d^4p_1}{(2\pi)^4}V_{1\mu\nu}D^{\mu\rho}(K^*)V_{2\rho}D(\kappa)V_{3\sigma}D^{\nu\sigma}(\bar{K}^*)\mathcal{F}(p_i^2),$$

$$V_{2\rho}=ig_{V_1K^*\kappa}\varepsilon^*_{V_1\rho},$$

$$V_{3\sigma}=ig_{V_2\bar{K}^*\kappa}\varepsilon^*_{V_2\sigma}.$$

- $[P,\ K,\ \bar{K}^*,\ (K)]$

  The amplitude for the $[P,\ K,\ \bar{K}^*,\ (K)]$ loop is

$$i\mathcal{M}=\int\frac{d^4p_1}{(2\pi)^4}V_{1\mu}D(K)V_2D^{\mu\nu}(\bar{K}^*)V_{3\nu}D(K)\mathcal{F}(p_i^2),$$

$$V_{1\mu}=ig_{DK\bar{K}^*}(p_D+p_1)_\mu,$$

$$V_2=ig_{V_1K\bar{K}}(p_1+p_2)_\rho\varepsilon^{\rho*}_{V_1}.$$

- $[P,\ K^*,\ \bar{K},\ (K)]$

  The amplitude for the $[P,\ K^*,\ \bar{K},\ (K)]$ loop is

$$i\mathcal{M} = \int \frac{d^4p_1}{(2\pi)^4} V_{1\sigma} D^{\sigma\mu}(K^*) V_{2\mu} D(K) V_3 D(\bar{K}) \mathcal{F}(p_i^2),$$

- $[P,\ K,\ \bar{K}^*,\ (K^*)]$

  The amplitude for the $[P,\ K,\ \bar{K}^*,\ (K^*)]$ loop is

$$i\mathcal{M} = \int \frac{d^4p_1}{(2\pi^4)} V_{1\nu} D(K) V_{2\rho} D^{\rho\sigma}(K^*) V_{3\nu'\sigma} D^{\nu\nu'}(\bar{K}^*) \mathcal{F}(p_i^2),$$

- $[P,\ K^*,\ \bar{K},\ (K^*)]$

  The amplitude for the $[P,\ K^*,\ \bar{K},\ (K^*)]$ loop is

$$i\mathcal{M} = \int \frac{d^4p_1}{(2\pi)^4} V_{1\sigma} D^{\sigma\mu}(K^*) V_{2\mu\rho} D^{\rho\nu}(K^*) V_{3\nu} D(\bar{K}) \mathcal{F}(p_i^2),$$

S wave loop amplitudes:

- $[S,\ K^*,\ \bar{K}^*,\ (K)]$

  The amplitude for the $[S,\ K^*,\ \bar{K}^*,\ (K)]$ loop is

$$i\mathcal{M} = \int \frac{d^4p_1}{(2\pi)^4} V_1 D^{\mu\rho}(K^*) V_{2\mu} D(K) V_3^{\nu} D_{\nu\rho}(\bar{K}^*) \mathcal{F}(p_i^2), \qquad V_1 = i g_{DK^*\bar{K}^*}.$$

- $[S,\ K^*,\ \bar{K}^*,\ (K^*)]$

  The amplitude for the $[P,\ K^*,\ \bar{K}^*,\ (K^*)]$ loop is

$$i\mathcal{M} = \int \frac{d^4p_1}{(2\pi)^4} V_1 D^{\mu\lambda}(K^*) V_{2\mu\rho} D^{\rho\sigma}(K^*) V_{3\sigma}^{\nu} D_{\lambda\nu}(\bar{K}^*) \mathcal{F}(p_i^2),$$

- $[S,\ K^*,\ \bar{K}^*,\ (\kappa)]$

  The amplitude for the $[S,\ K^*,\ \bar{K}^*,\ (\kappa)]$ loop is

$$i\mathcal{M} = \int \frac{d^4p_1}{(2\pi)^4} V_1 D^{\mu\rho}(K^*) V_{2\rho} D(\kappa) V_3^{\sigma} D_{\mu\sigma}(\bar{K}^*) \mathcal{F}(p_i^2),$$

- $[S,\ K,\ \bar{K},\ (K)]$

  The amplitude for the $[S,\ K,\ \bar{K},\ (K)]$ loop is

$$i\mathcal{M} = \int \frac{d^4p_1}{(2\pi)^4} V_1 D(K) V_2 D(K) V_3 D(\bar{K}) \mathcal{F}(p_i^2),$$

- $[S,\ K,\ \bar{K},\ (K^*)]$

$$i\mathcal{M} = \int \frac{d^4p_1}{(2\pi)^4} V_1 D(K) V_{2\mu} D^{\mu\nu}(K^*) V_{3\nu} D(\bar{K}) \mathcal{F}(p_i^2)$$

Results and discussions

Tree-level couplings for $D^0 \to VV$ via the DE transition, and long-distance couplings from the intermediate $D^0 \to PP$ and VP in the FSIs:

VV Modes	b.r. of expt.	$g_{\rm DE}^{(\rm PC)}$ [GeV^{-1}]	$g_{\rm DE}^{(\rm PV)}$ [GeV]
$K^{*-}\rho^+$	$(65.0 \pm 25.0) \times 10^{-3}$	2.52 ± 0.43	4.70 ± 0.63
$K^{*+}K^{*-}$	-	2.81 ± 0.60	5.27 ± 0.89
$\rho^+\rho^-$	-	3.20 ± 0.88	4.40 ± 0.80
PP/VP Modes	b.r. of expt.	$g^{(\rm PC)}$	$g^{(\rm PV)}$ [GeV]
$K^-\pi^+$	$(3.95 \pm 0.03)\%$	0	2.64 ± 0.01
K^+K^-	$(4.08 \pm 0.06) \times 10^{-3}$	0	3.84 ± 0.03
$\pi^+\pi^-$	$(1.45 \pm 0.02) \times 10^{-3}$	0	2.19 ± 0.02
$K^{*-}\pi^+$	$(6.93 \pm 1.20)\%$	1.29 ± 0.11	0
ρ^+K^-	$(11.20 \pm 0.70)\%$	1.54 ± 0.05	0
$K^{*-}K^+$	$(1.86 \pm 0.30) \times 10^{-3}$	1.16 ± 0.09	0
$K^{*+}K^-$	$(5.67 \pm 0.90) \times 10^{-3}$	2.02 ± 0.16	0
$\rho^-\pi^+$	$(5.15 \pm 0.25) \times 10^{-3}$	1.23 ± 0.03	0
$\rho^+\pi^-$	$(1.01 \pm 0.04)\%$	1.72 ± 0.03	0

Couplings are determined by the NRCQM.

The couplings for $D^0 \to PP/VP$ are determined by exp. data. They can also contribute to the VV decays via the FSIs.

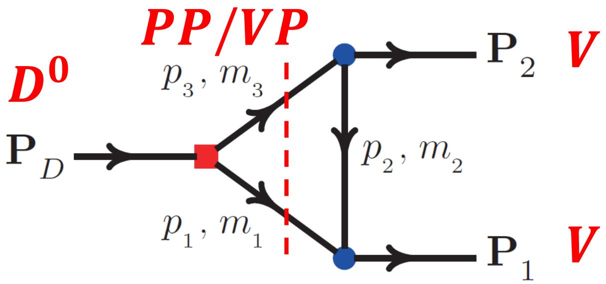

Cut-off parameter α dependence of the partial-wave b.r.s of $D^0 \to \phi\rho^0$, and polarization b.r.s of $D^0 \to \phi\omega$, respectively. The solid lines stand for the total b.r.s.

$D^0 \to \phi\rho^0$

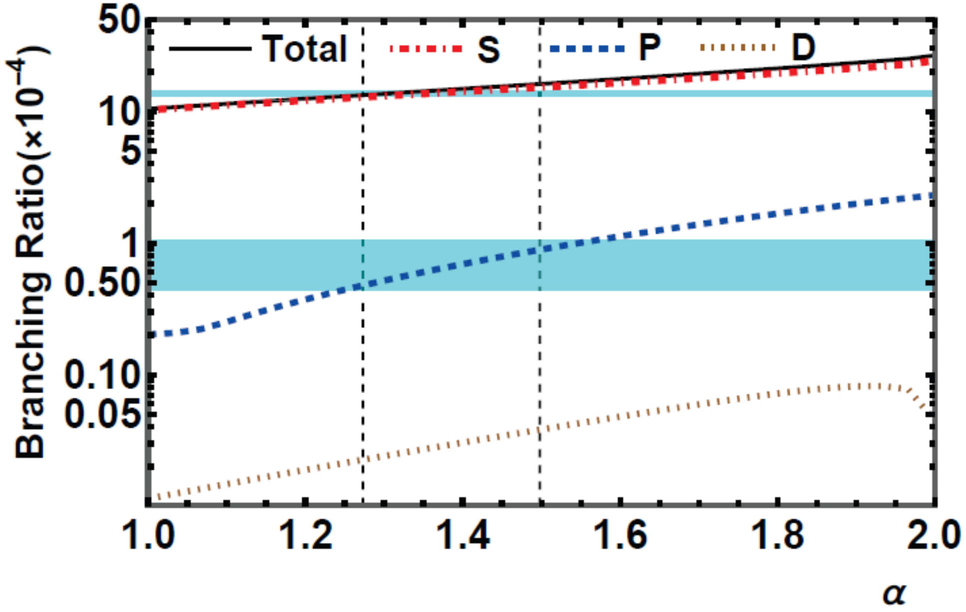

$D^0 \to \phi\omega$

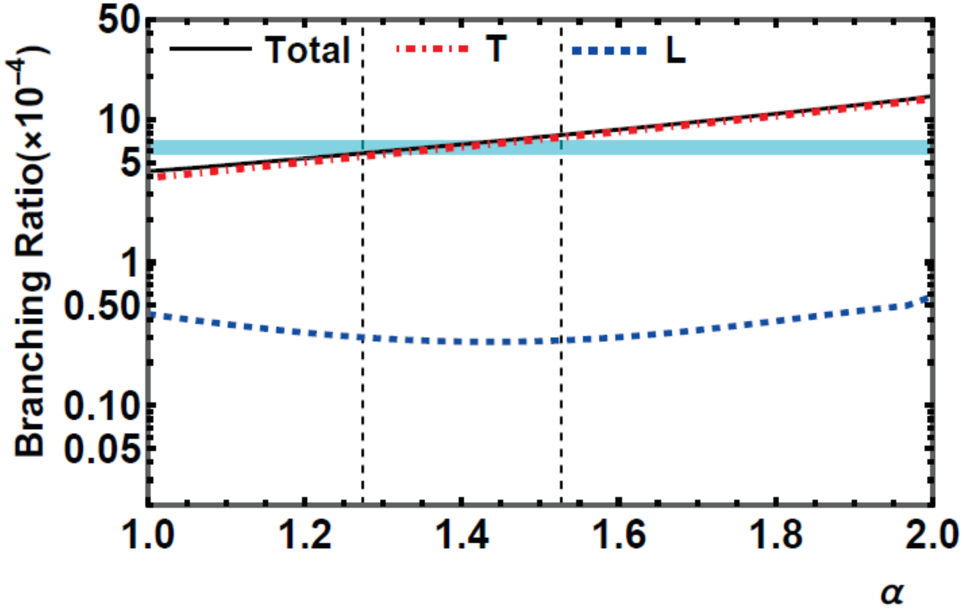

Form factor : $\mathcal{F}(p_i^2) = \prod_i (\frac{\Lambda_i^2 - m_i^2}{\Lambda_i^2 - p_i^2})$, with $\Lambda_i \equiv m_i + \alpha\Lambda_{QCD}$, and $\Lambda_{QCD} = 220$ MeV, and $\alpha \simeq 1 \sim 2$.

Determine the IC amplitudes by data

Decay channels	Amplitudes
$K^{*-}\rho^+$	$[g_{\rm DE}^{\rm (P)} + e^{i\theta} g_{{\rm IC}(s\bar{d})}^{\rm (P)}]V_{cs}V_{ud}$
$\bar{K}^{*0}\rho^0$	$\frac{1}{\sqrt{2}}[g_{\rm CS}^{\rm (P)} - e^{i\theta} g_{{\rm IC}(s\bar{d})}^{\rm (P)}]V_{cs}V_{ud}$
$\bar{K}^{*0}\omega$	$\frac{1}{\sqrt{2}}[g_{\rm CS}^{\rm (P)} + e^{i\theta} g_{{\rm IC}(s\bar{d})}^{\rm (P)}]V_{cs}V_{ud}$
$K^{*+}K^{*-}$	$[g_{\rm DE}^{\rm (P)} + e^{i\theta} g_{{\rm IC}(s\bar{s})}^{\rm (P)}]V_{cs}V_{us}$
$K^{*0}\bar{K}^{*0}$	$e^{i\theta}[g_{{\rm IC}(s\bar{s})}^{\rm (P)} V_{cs}V_{us} + g_{{\rm IC}(d\bar{d})}^{\rm (P)} V_{cd}V_{ud}]$

CF	Experiments	Fitted values ($\alpha = 1.4 \pm 0.14$)
$K^{*-}\rho^+$	$(6.5 \pm 2.5)\%$[33]	$(6.58^{+0.14}_{-0.10})\%$
$\bar{K}^{*0}\rho^0$	$(1.515 \pm 0.075)\%$[34] $(1.59 \pm 0.35)\%$[18]	$(1.53^{+0.24}_{-0.26})\%$
$\bar{K}^{*0}\rho^0[T]$	$(1.8 \pm 0.6)\%$[18]	$(1.10^{+0.13}_{-0.16})\%$
$\bar{K}^{*0}\omega$	$(1.1 \pm 0.5)\%$[33]	$(0.95^{+0.04}_{-0.06})\%$

SCS	Experiments	Fitted values ($\alpha = 1.4 \pm 0.14$)
$K^{*0}\bar{K}^{*0}[S]$	$(5.04 \pm 0.30) \times 10^{-4}$[21]	$(5.31^{+3.02}_{-2.04}) \times 10^{-4}$
$K^{*0}\bar{K}^{*0}[P]$	$(2.70 \pm 0.18) \times 10^{-4}$[21]	$(2.82^{+0.08}_{-0.13}) \times 10^{-4}$
$K^{*0}\bar{K}^{*0}[D]$	$(1.06 \pm 0.09) \times 10^{-4}$[21]	$(0.11^{+0.04}_{-0.03}) \times 10^{-4}$
$K^{*0}\bar{K}^{*0}[\rm Total]$	$(8.80 \pm 0.36) \times 10^{-4}$[21]	$(8.31^{+3.18}_{-2.24}) \times 10^{-4}$

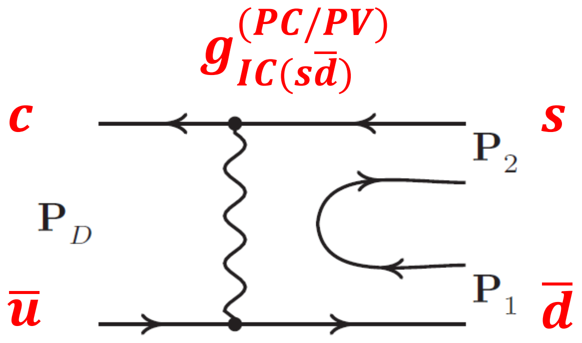

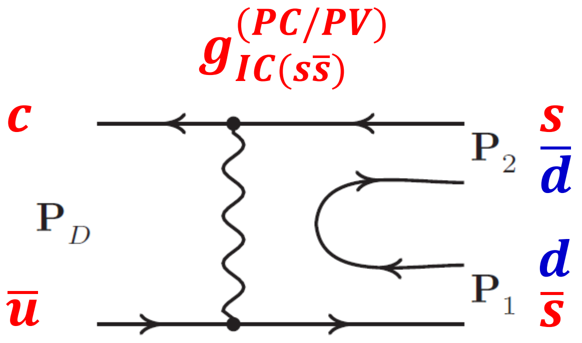

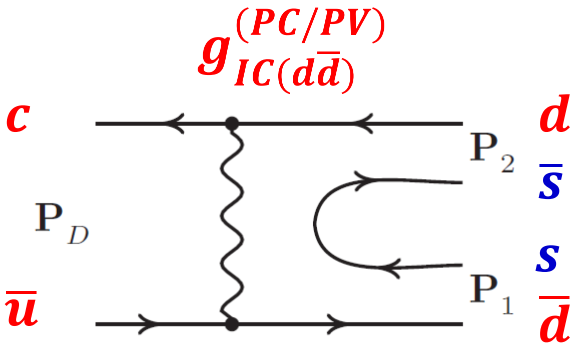

$$\begin{cases} g_{{\rm IC}(s\bar{d})}^{\rm (PC)} \simeq (0.2 \sim 0.5) \times 10^{-6}\ {\rm GeV}^{-1} \\ g_{{\rm IC}(s\bar{d})}^{\rm (PV)} \simeq (2.5 \sim 3.0) \times 10^{-6}\ {\rm GeV} \end{cases}$$

$$\begin{cases} g_{{\rm IC}(s\bar{s})}^{\rm (PC)} \simeq g_{{\rm IC}(d\bar{d})}^{\rm (PC)} \simeq (1.0 \sim 1.2) \times 10^{-6}\ {\rm GeV}^{-1} \\ g_{{\rm IC}(s\bar{s})}^{\rm (PV)} \simeq g_{{\rm IC}(d\bar{d})}^{\rm (PV)} \simeq (0.8 \sim 1.0) \times 10^{-6}\ {\rm GeV} \end{cases}$$

Numerical results in comparison with the data

- (purple) Leading processes with the DE trans.
- (blue) CF trans. with CS
- (yellow) SCS trans. with CS

in unit of ($\times 10^{-3}$)

Process		Experiments	b.r.s *with* FSIs	b.r.s *without* FSIs
$K^{*-}\rho^+$	T	-	$57.92^{+0.96}_{-0.59}$	47.59
	L	-	$7.88^{+0.43}_{-0.43}$	4.58
	Total	65.0 ± 25.0[31]	$65.80^{+1.39}_{-1.02}$	52.17
$\bar{K}^{*0}\rho^0$	T	18.0 ± 6.0[18]	$10.95^{+1.28}_{-1.55}$	12.36
	L	-	$4.34^{+1.09}_{-1.09}$	5.31
	Total	15.9 ± 3.5[18] 15.15 ± 0.75 [32]	$15.29^{+2.37}_{-2.64}$	17.68
$\bar{K}^{*0}\omega$	T	-	$6.85^{+0.36}_{-0.51}$	7.52
	L	-	$2.62^{+0.09}_{-0.08}$	2.76
	Total	11.0 ± 5.0[31]	$9.48^{+0.45}_{-0.59}$	10.28
$K^{*+}K^{*-}$	T	-	$6.22^{+0.26}_{-0.37}$	4.02
	L	-	$2.93^{+0.09}_{-0.16}$	1.83
	Total	-	$9.15^{+0.35}_{-0.53}$	5.86
$K^{*0}\bar{K}^{*0}$	**S**	0.50 ± 0.03[21]	$0.56^{+0.25}_{-0.15}$	0.92
	P	0.27 ± 0.02[21]	$0.27^{+0.006}_{-0.009}$	0.30
	D	0.11 ± 0.01[21]	$0.01^{+0.004}_{-0.003}$	0.006
	T	-	$0.58^{+0.13}_{-0.08}$	0.84
	L	-	$0.27^{+0.10}_{-0.07}$	0.39
	Total	0.88 ± 0.04[21]	$0.84^{+0.24}_{-0.15}$	1.23

Decay channels	Amplitudes
$K^{*-}\rho^+$	$[g^{(P)}_{\rm DE} + e^{i\theta} g^{(P)}_{{\rm IC}(s\bar{d})}]V_{cs}V_{ud}$
$\bar{K}^{*0}\rho^0$	$\frac{1}{\sqrt{2}}[g^{(P)}_{\rm CS} - e^{i\theta} g^{(P)}_{{\rm IC}(s\bar{d})}]V_{cs}V_{ud}$
$\bar{K}^{*0}\omega$	$\frac{1}{\sqrt{2}}[g^{(P)}_{\rm CS} + e^{i\theta} g^{(P)}_{{\rm IC}(s\bar{d})}]V_{cs}V_{ud}$
$K^{*+}K^{*-}$	$[g^{(P)}_{\rm DE} + e^{i\theta} g^{(P)}_{{\rm IC}(s\bar{s})}]V_{cs}V_{us}$
$K^{*0}\bar{K}^{*0}$	$e^{i\theta}[g^{(P)}_{{\rm IC}(s\bar{s})}V_{cs}V_{us} + g^{(P)}_{{\rm IC}(d\bar{d})}V_{cd}V_{ud}]$

- The long-distance FSIs are crucial and evident.
- The difference between $\bar{K}^{*0}\rho^0$ and $\bar{K}^{*0}\omega$ indicates the non-negligible contributions from the IC transitions. About 10% corrections from the long-distance FSIs are expected.

Numerical results in comparison with the data

in unit of $(\times 10^{-3})$

Process		Experiments	b.r.s *with* FSIs	b.r.s *without* FSIs
$\rho^+\rho^-$	T	-	$4.19^{+0.31}_{-0.31}$	5.44
	L	-	$0.91^{+0.09}_{-0.04}$	1.36
	Total	-	$5.10^{+0.40}_{-0.35}$	6.81
$\rho^0\rho^0$	**S**	0.18 ± 0.13[21]	$0.38^{+0.42}_{-0.26}$	0.49
	P	0.53 ± 0.13[21]	$0.42^{+0.06}_{-0.06}$	0.23
	D	0.62 ± 0.30[21]	$0.04^{+0.02}_{-0.02}$	0.01
	T	0.56 ± 0.07[19]	$0.67^{+0.28}_{-0.20}$	0.48
	L	1.27 ± 0.10[19]	$0.18^{+0.22}_{-0.14}$	0.25
	Total	1.85 ± 0.13[19] 1.33 ± 0.35[21]	$0.85^{+0.49}_{-0.34}$	0.73
$\omega\omega$	T	-	$0.050^{+0.005}_{-0.004}$	0.019
	L	-	$0.028^{+0.0001}_{-0.002}$	0.00065
	Total	-	$0.078^{+0.005}_{-0.006}$	0.020
$\rho^0\omega$	T	-	$1.03^{+0.01}_{-0.03}$	0.84
	L	-	$0.09^{+0.009}_{-0.004}$	0.13
	Total	-	$1.11^{+0.013}_{-0.024}$	0.97
$\phi\rho^0$	**S**	1.40 ± 0.12[21]	$1.41^{+0.16}_{-0.14}$	0.48
	P	0.08 ± 0.04[21]	$0.07^{+0.03}_{-0.02}$	0.05
	D	0.08 ± 0.03[21]	$0.003^{+0.001}_{-0.001}$	~ 0
	T	-	$1.01^{+0.14}_{-0.12}$	0.37
	L	-	$0.48^{+0.05}_{-0.04}$	0.16
	Total	1.56 ± 0.13[21]	$1.48^{+0.19}_{-0.17}$	0.53
$\phi\omega$	T	0.65 ± 0.10[20]	$0.64^{+0.12}_{-0.10}$	0.34
	L	~ 0 [20]	$0.03^{+0.001}_{-0.002}$	0.15
	Total	0.65 ± 0.10[20]	$0.67^{+0.12}_{-0.10}$	0.49

Leading processes with the DE trans.

CF trans. with CS

SCS trans. with CS

$\rho^+\rho^-$	$[g^{(P)}_{\mathrm{DE}} + e^{i\theta} g^{(P)}_{\mathrm{IC}(d\bar{d})}] V_{cd} V_{ud}$
$\rho^0\rho^0$	$\frac{1}{2}[-g^{(P)}_{\mathrm{CS}} + e^{i\theta} g^{(P)}_{\mathrm{IC}(d\bar{d})}] V_{cd} V_{ud}$
$\omega\omega$	$\frac{1}{2}[g^{(P)}_{\mathrm{CS}} + e^{i\theta} g^{(P)}_{\mathrm{IC}(d\bar{d})}] V_{cd} V_{ud}$
$\rho^0\omega$	$-\frac{1}{2} e^{i\theta} g^{(P)}_{\mathrm{IC}(d\bar{d})} V_{cd} V_{ud}$
$\phi\rho^0$	$\frac{1}{\sqrt{2}} g^{(P)}_{\mathrm{CS}} V_{cs} V_{us}$
$\phi\omega$	$\frac{1}{\sqrt{2}} g^{(P)}_{\mathrm{CS}} V_{cs} V_{us}$

- Without the long-distance FSI contributions it is impossible to account for the difference between the $\phi\rho^0$ and $\phi\omega$ decays.
- The suppression of the $\omega\omega$ channel indicates the relative strength between the CS and IC transitions.
- The $\rho^0\omega$ channel is dominantly driven by the IC transition for which the experimental measurement will provide a direct constraint on this mechanism.

Further implications of the long-distance dynamics

- We can presumably learn something from the D meson weak radiative decays:

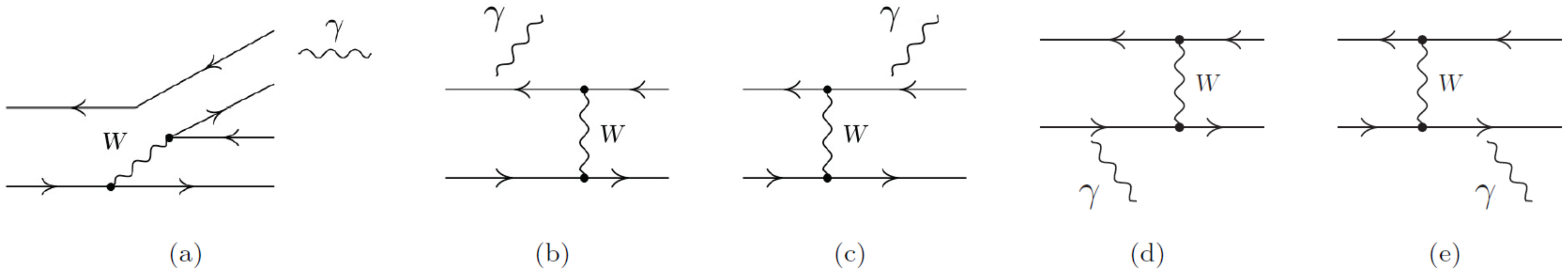

- Vector meson dominance (VMD) provides a self-contained prescription for $D \to V\gamma$
- Manifestation of long-distance mechanisms are anticipated

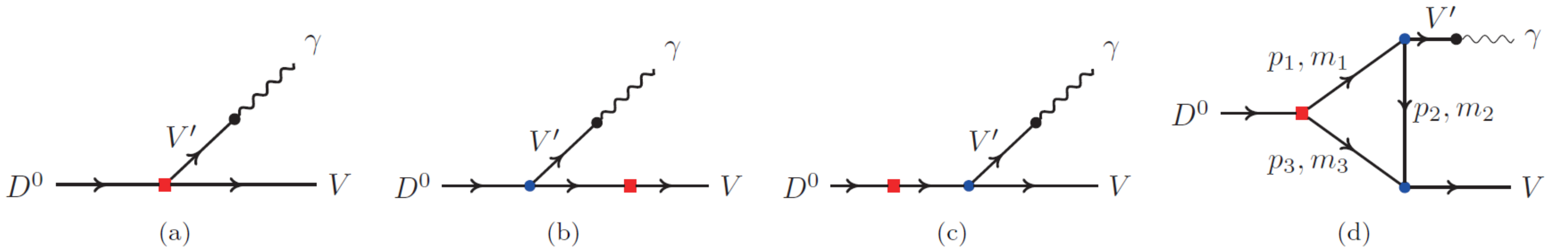

$D^0 \to V\gamma$

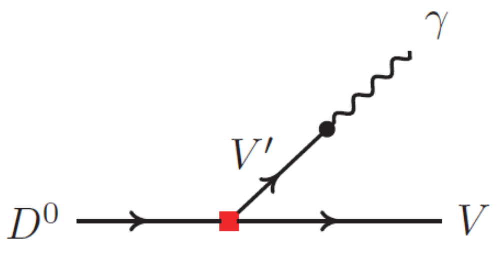

(a)

Tree-level amplitudes: $i\mathcal{M}^{(\mathrm{P})}_{\mathrm{CS}} = \langle V_1(\mathbf{P}_1; J_1, J_{1z}) V_2(\mathbf{P}_2; J_2, J_{2z}) | \hat{H}^{(\mathrm{P})}_{W,1\to 3} | D^0(\mathbf{P}_D; J_i, J_{iz})\rangle,$

$$\begin{cases} i\mathcal{M}^{(\mathrm{PC})}_{T(a)} = i g^{(\mathrm{PC})}_{DV\gamma} \epsilon_{\alpha\beta\delta\lambda} p^{\alpha}_{\gamma} p^{\beta}_{V} \varepsilon^{\delta}_{\gamma} \varepsilon^{\lambda}_{V}, \\ i\mathcal{M}^{(\mathrm{PV})}_{T(a)} = -i g^{(\mathrm{PV})}_{DV\gamma} \varepsilon^{\mu}_{\gamma} \varepsilon_{V\mu}, \end{cases}$$

$$\begin{cases} g^{(\mathrm{P})}_{DV\gamma} = -i g^{(\mathrm{P})}_{DVV'} \dfrac{e m^2_{V'}}{f_{V'}} G_{V'}, \\ G_{V'} \equiv \dfrac{-i}{p^2_{\gamma} - m^2_{V'} + i m_{V'}\Gamma_{V'}} = \dfrac{-i}{-m^2_{V'} + i m_{V'}\Gamma_{V'}} \end{cases}$$

Modes	Tree amplitudes (Fig. 2(a))
$\bar{K}^{*0}\gamma$	$\frac{1}{\sqrt{2}} g^{(\mathrm{P})}_{W(\mathrm{CS})} V_{cs} V_{ud} \frac{e m^2_{\rho^0}}{f_{\rho^0}} G_{\rho^0} + \frac{1}{\sqrt{2}} g^{(\mathrm{P})}_{W(\mathrm{CS})} V_{cs} V_{ud} \frac{e m^2_{\omega}}{f_{\omega}} G_{\omega}$
$\phi\gamma$	$\frac{1}{\sqrt{2}} g^{(\mathrm{P})}_{W(\mathrm{CS})} V_{cs} V_{us} \frac{e m^2_{\rho^0}}{f_{\rho^0}} G_{\rho^0} + \frac{1}{\sqrt{2}} g^{(\mathrm{P})}_{W(\mathrm{CS})} V_{cs} V_{us} \frac{e m^2_{\omega}}{f_{\omega}} G_{\omega}$
$\rho^0\gamma$	$-\frac{1}{2} g^{(\mathrm{P})}_{W(\mathrm{CS})} V_{cd} V_{ud} \frac{e m^2_{\rho^0}}{f_{\rho^0}} G_{\rho^0} + \frac{1}{\sqrt{2}} g^{(\mathrm{P})}_{W(\mathrm{CS})} V_{cs} V_{us} \frac{e m^2_{\phi}}{f_{\phi}} G_{\phi}$
$\omega\gamma$	$\frac{1}{2} g^{(\mathrm{P})}_{W(\mathrm{CS})} V_{cd} V_{ud} \frac{e m^2_{\omega}}{f_{\omega}} G_{\omega} + \frac{1}{\sqrt{2}} g^{(\mathrm{P})}_{W(\mathrm{CS})} V_{cs} V_{us} \frac{e m^2_{\phi}}{f_{\phi}} G_{\phi}$

Decay channels	$D^0 \to \bar{K}^{*0}\rho^0/\bar{K}^{*0}\rho^0$	$D^0 \to \phi\rho^0/\phi\omega$	$D^0 \to \rho^0\rho^0/\omega\omega$
$g^{(\mathrm{PC})\mathbb{T}}_{W(\mathrm{CS})}$ [GeV^{-1}]	1.47 ± 0.31	1.63 ± 0.34	1.31 ± 0.35
$g^{(\mathrm{PV})\mathbb{T}}_{W(\mathrm{CS})}$ [GeV]	1.71 ± 0.29	1.90 ± 0.32	1.53 ± 0.33
$g^{(\mathrm{PV})\mathbb{L}}_{W(\mathrm{CS})}$ [GeV]	1.15 ± 0.19	1.64 ± 0.28	0.81 ± 0.02

Channel	Total width of V'	BR($V' \to e^+e^-$)	$e/f_{V'}(\times 10^{-2})$
$\phi \to e^+e^-$	4.25 MeV	$(2.98 \pm 0.03) \times 10^{-4}$	-2.26
$\rho^0 \to e^+e^-$	147.4 MeV	$(4.72 \pm 0.05) \times 10^{-5}$	6.07
$\omega \to e^+e^-$	8.68 MeV	$(7.38 \pm 0.22) \times 10^{-5}$	1.83
$J/\psi \to e^+e^-$	92.6 keV	$(5.97 \pm 0.032)\%$	2.71

Pole terms:

$$\mathcal{M}_I^{(\mathrm{P})}(D \to V\gamma) = \sum_n \langle V | H_{W,2\to 2}^{(\mathrm{P})} \frac{i}{m_V^2 - m_{D_n^*}^2 + i m_{D_n^*}\Gamma_{D_n^*}} | D_n^* \rangle \langle D_n^* | H_{EM} | D \rangle,$$

$$\mathcal{M}_{II}^{(\mathrm{P})}(D \to V\gamma) = \sum_n \langle V | H_{EM} \frac{i}{m_D^2 - m_{P_n}^2 + i m_{P_n}\Gamma_{P_n}} | P_n \rangle \langle P_n | H_{W,2\to 2}^{(\mathrm{P})} | D \rangle$$

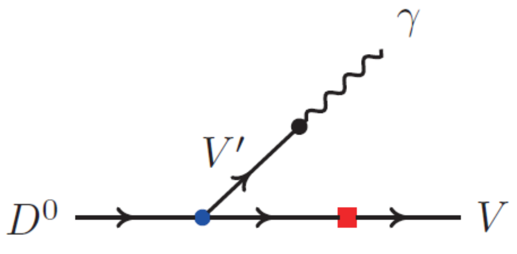

(b)

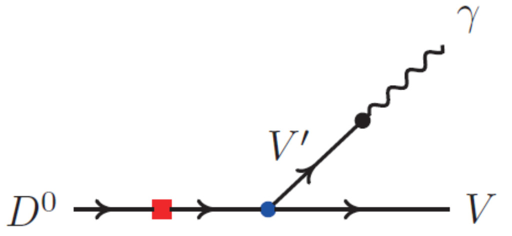

(c)

- PC transition amplitude

$$i\mathcal{M}_I^{(\mathrm{PC})} = (i\mathcal{M}_{D\to V'D^*}) G_{V'} (i\mathcal{M}_{V'\gamma}) G_{D^*} (i\mathcal{M}_{D^*V})$$

$$= (i g_{DD^*V'} \epsilon_{\alpha\beta\mu\lambda} i p_{V'}^\alpha i p_{D^*}^\beta) \frac{-i(g^{\mu\nu} - \frac{p_{V'}^\mu p_{V'}^\nu}{p_{V'}^2})}{p_{V'}^2 - m_{V'}^2 + i m_{V'}\Gamma_{V'}} \left(\frac{i e m_{V'}^2}{f_{V'}} \varepsilon_\gamma^\nu\right) \frac{-i(g^{\lambda\delta} - \frac{p_{D^*}^\lambda p_{D^*}^\delta}{p_{D^*}^2})}{p_{D^*}^2 - m_{D^*}^2 + i m_{D^*}\Gamma_{D^*}} (i g_{D^*V}^{(\mathrm{PC})} \varepsilon_V^\delta)$$

$$\times\, \delta(p_{V'} - p_\gamma)\delta(p_{D^*} - p_V)$$

$$= i\epsilon_{\alpha\beta\mu\lambda} p_\gamma^\alpha p_V^\beta \varepsilon_\gamma^\mu \varepsilon_V^\lambda \left(g_{DD^*V'} \frac{e m_{V'}^2}{f_{V'}} \frac{-i}{p_\gamma^2 - m_{V'}^2 + i m_{V'}\Gamma_{V'}} g_{D^*V}^{(\mathrm{PC})} \frac{-i}{m_V^2 - m_{D^*}^2 + i m_{D^*}\Gamma_{D^*}}\right)$$

$$= i g_{DV\gamma}^{(\mathrm{PC})} \epsilon_{\alpha\beta\mu\lambda} p_\gamma^\alpha p_V^\beta \varepsilon_\gamma^\mu \varepsilon_V^\lambda,$$

where $g_{DV\gamma}^{(\mathrm{PC})} = g_{DD^*(1^-)V'} \frac{e m_{V'}^2}{f_{V'}} G_{V'} g_{D^*V}^{(\mathrm{PC})} \mathbb{G}_{V,D^*}$, $G_V \equiv \frac{-i}{p_\gamma^2 - m_V^2 + i m_V\Gamma_V} = \frac{-i}{-m_V^2 + i m_V\Gamma_V}$, and $\mathbb{G}_{V,V'} \equiv \frac{-i}{m_V^2 - m_{V'}^2 + i m_{V'}\Gamma_{V'}}$.

Triangle loop amplitudes:

$$i\mathcal{M}^{(\mathrm{P})}_{loop} = \sum_{\mathbb{K}} \tilde{\mathcal{I}}[(\mathrm{P}),\ K^{*+},\ K^{*-},\ (\mathbb{K})],$$

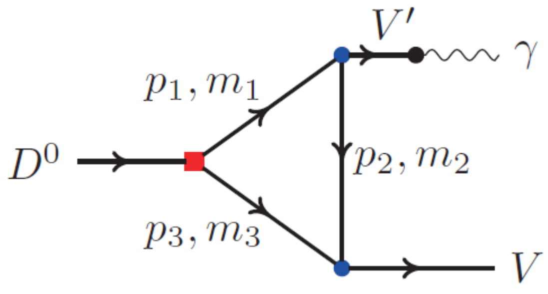

(d)

Taking the PC loop transition $[(\mathrm{PC});\ K^*,\ \bar{K}^*,\ (K)]$ as an example, the loop integral is:

$$\tilde{\mathcal{I}}[(\mathrm{PC});\ K^*,\ \bar{K}^*,\ (K)] = \int \frac{d^4 p_1}{(2\pi)^4} V_{1\mu\nu} D^{\mu\mu'}(K^*) V_{2\mu'} D(K) V_{3\nu'} D^{\nu\nu'}(\bar{K}^*) \mathcal{F}(p_i^2),$$

where the vertex functions have compact forms as follows:

$$V_{1\mu\nu} = -i g^{(\mathrm{P})}_{W(\mathrm{SD})} V_{cs} V_{us} \epsilon_{\alpha\beta\mu\nu} p_1^{\alpha} p_3^{\beta},$$
$$V_{2\mu'} = i g_{K^*\bar{K}\gamma} \epsilon_{\alpha_1\beta_1\mu'\delta} p_1^{\alpha_1} p_\gamma^{\beta_1} \varepsilon_\gamma^{*\delta},$$
$$V_{3\nu'} = i g_{V\bar{K}^*K} \epsilon_{\alpha_2\beta_2\nu'\lambda} p_3^{\alpha_2} p_V^{\beta_2} \varepsilon_V^{*\lambda}\ ,$$

$$D^{\mu\mu'}(K^*) = \frac{-i(g^{\mu\mu'} - \frac{p^\mu p^{\mu'}}{p^2})}{p^2 - m_{K^*}^2 + i\epsilon},$$
$$D(K) = \frac{i}{p^2 - m_K^2 + i\epsilon}.$$

Calculated b.r.s of each type of the hadronic loop diagrams in units of 10^{-5} with the cut-off parameter $\alpha = 1$ and $\alpha = 2$.

Diagrams	Decay channels	$\alpha = 1$			$\alpha = 2$		
		(PC)	(PV)	(PC)+(PV)	(PC)	(PV)	(PC)+(PV)
$[K^{*+}, K^{*-}, (K^+)]$	$\phi\gamma$	5.79×10^{-5}	1.14×10^{-2}	1.15×10^{-2}	5.33×10^{-4}	5.24×10^{-2}	5.29×10^{-2}
	$\rho^0\gamma$	1.72×10^{-5}	5.21×10^{-3}	5.23×10^{-3}	1.97×10^{-4}	2.79×10^{-2}	2.81×10^{-2}
	$\omega\gamma$	1.74×10^{-5}	5.22×10^{-3}	5.23×10^{-3}	1.98×10^{-4}	2.79×10^{-2}	2.81×10^{-2}
$[K^{*+}, K^{*-}, (K^{*+})]$	$\phi\gamma$	3.29×10^{-3}	0.61	0.61	2.23×10^{-2}	2.15	2.17
	$\rho^0\gamma$	1.10×10^{-3}	0.18	0.18	9.93×10^{-3}	0.84	0.85
	$\omega\gamma$	1.11×10^{-3}	0.18	0.18	9.92×10^{-3}	0.85	0.86
$[K^{*-}, \rho^+, (K^-)]$	$\bar{K}^{*0}\gamma$	1.39×10^{-3}	2.73×10^{-2}	2.87×10^{-2}	1.11×10^{-2}	8.95×10^{-2}	0.10
$[K^{*-}, \rho^+, (K^{*-})]$	$\bar{K}^{*0}\gamma$	7.24×10^{-2}	1.18	1.25	0.44	3.60	4.04
$[\rho^+, K^{*-}, (\pi^+)]$	$\bar{K}^{*0}\gamma$	1.18×10^{-4}	1.42×10^{-2}	1.43×10^{-2}	2.33×10^{-3}	5.98×10^{-2}	6.21×10^{-2}
$[\rho^+, K^{*-}, (\rho^+)]$	$\bar{K}^{*0}\gamma$	0.12	1.78	1.91	0.72	5.20	5.92

Calculated b.r.s containing both tree and loop contributions in units of 10^{-5} for the four radiative weak decays $D^0 \to V\gamma$ ($V = \bar{K}^{*0}$, ϕ, ρ^0, ω). The uncertainties are given by $\alpha = 1.3 \pm 0.13$.

	$D^0 \to \bar{K}^{*0}\gamma$	$D^0 \to \phi\gamma$	$D^0 \to \rho^0\gamma$	$D^0 \to \omega\gamma$
Experimental data	$32.8 \pm 2.0 \pm 2.7$ [5] $46.6 \pm 2.1 \pm 2.1$ [6]	$2.78 \pm 0.32 \pm 0.27$ [5] $2.76 \pm 0.19 \pm 0.10$ [6]	$1.77 \pm 0.30 \pm 0.07$ [6]	< 24 [4]
PDG average [21]	41 ± 7	2.81 ± 0.19	1.82 ± 0.32	< 24
Burdman [10]	$7 \sim 12$	$0.1 \sim 3.4$	$0.1 \sim 0.5$	~ 0.2
Biswas [13]	$4.6 \sim 18$	$0.48 \sim 0.64$	$0.512 \sim 1.8$	$0.32 \sim 0.9$
Fajfer [11]	$6 \sim 36$	$0.4 \sim 1.9$	$0.1 \sim 1$	$0.1 \sim 0.9$
Shen [15]	19^{+7+1}_{-6-1}	$3.2^{+1.3+0.3}_{-1.0-0.0}$	$1.1^{+0.4+0.1}_{-0.4-0.1}$	$0.75^{+0.30+0.05}_{-0.25-0.04}$
de Boer [12]	$2.6 \sim 46$	$0.24 \sim 2.8$	$0.041 \sim 1.17$	$0.042 \sim 1.12$
Asthana [7]	0.86	-	-	-
Bajc [9]	$28 \sim 65$	-	-	-
Dias [27]	$15.5 \sim 34.4$	-	-	-
This work	$35.9^{+2.0}_{-2.2}$	$2.76^{+0.36}_{-0.35}$	$1.79^{+0.24}_{-0.22}$	$0.58^{+0.14}_{-0.13}$

4. Some insights into D meson decays

- The FSIs via $VV^{(DE)} \to VV^{(CS)}$ seems to be a natural explanation for the mysterious issues in $D^0 \to VV$, including the polarization puzzles.
- FSIs of the leading DE transitions can rescatter into the CS processes and produce significant interfering effects.
- The significant differences between the $\phi\rho^0$ and $\phi\omega$ decay channels can be understood.
- A combined analysis of the $\rho^0\rho^0, \omega\omega,$ and $\rho^0\omega$ channels will highlight the role played by the FSI mechanism.
- The leading processes, which involve the DE transitions, i.e. $D^0 \to K^{*-}\rho^+, K^{*+}K^{*-}, \rho^+\rho^-$, have not yet been measured! Polarization data for these decay channels will test the NRCQM inputs and further constrain both the short and long-distance transition mechanisms in $D^0 \to VV$.
- The D meson weak radiative decays may be useful for clarifying the long-distance mechansims.

Thanks for your attention!

Near-threshold coupled-channel effects

- Color screening effects? String breaking effects?

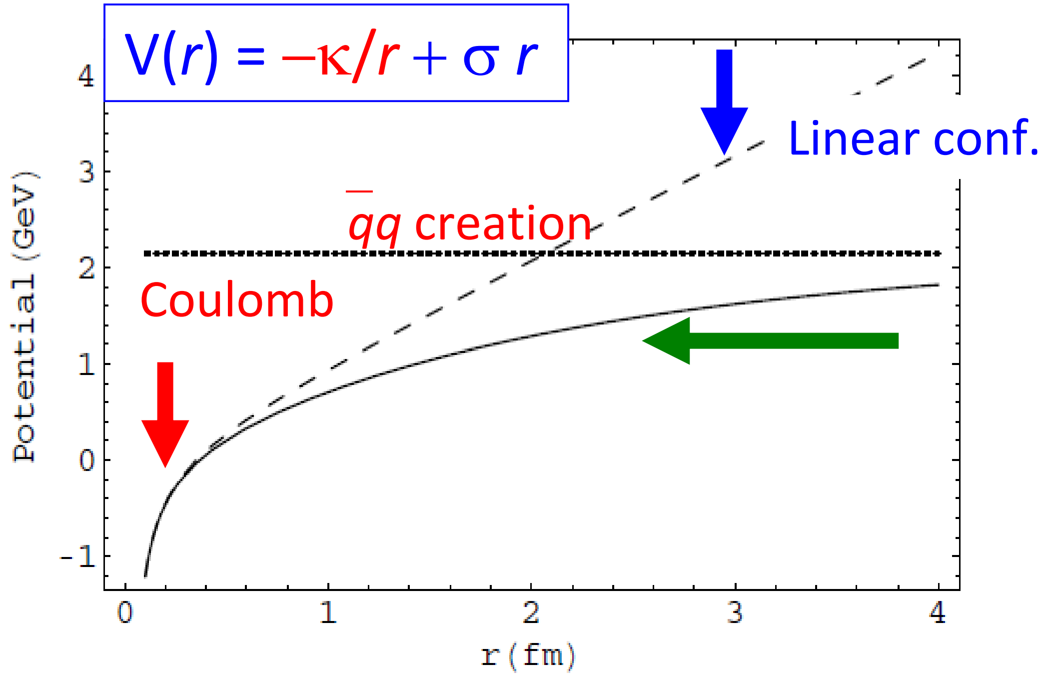

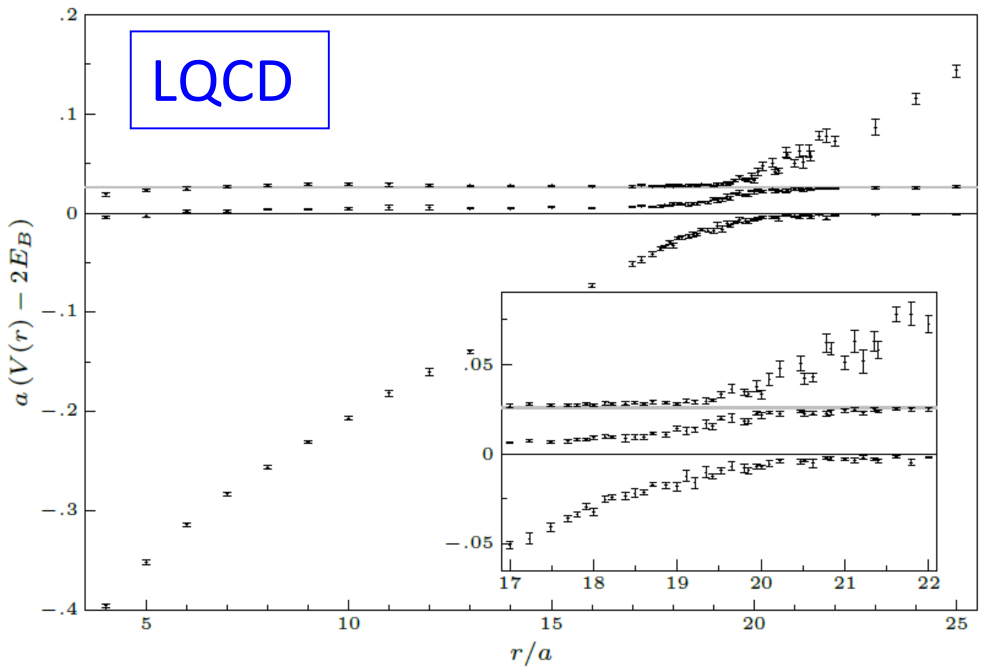

- The effect of vacuum polarization due to dynamical quark pair creation may be manifested by the strong coupling to open thresholds and compensated by that of the hadron loops, i.e. coupled-channel effects.

E. Eichten et al., PRD17, 3090 (1987)
E. J. Eichten, K. Lane, and C. Quigg, Phys. Rev. D 69, 094019 (2004)
B.-Q. Li and K.-T. Chao, Phys. Rev. D79, 094004 (2009);
T. Barnes and E. Swanson, Phys.Rev. C77, 055206 (2008)

Some interesting points to be made:

- The FSIs via $VV^{(DE)} \to VV^{(CS)}$ seems to be a natural explanation for the mysterious issues in $D^0 \to VV$, including the polarization puzzles.
- FSIs of the leading DE transitions can rescatter into the CS processes and produce significant interfering effects.
- The significant differences between the $\phi\rho^0$ and $\phi\omega$ decay channels can be understood.
- A combined analysis of the $\rho^0\rho^0, \omega\omega,$ and $\rho^0\omega$ channels will highlight the role played by the FSI mechanism.
- The leading processes, which involve the DE transitions, i.e. $D^0 \to K^{*-}\rho^+, K^{*+}K^{*-}, \rho^+\rho^-$, have not yet been measured. Polarization data for these decay channels will test the NRCQM inputs and further constrain both the short and long-distance transition mechanisms in $D^0 \to VV$.